JBC Papers in Press. Published on November 9, 2018 as Manuscript RA118.002896
The latest version is at http://www.jbc.org/cgi/doi/10.1074/jbc.RA118.002896

NFAT5 up-regulates expression of the kidney-specific ubiquitin ligase gene *Rnf183* under hypertonic conditions in inner-medullary collecting duct cells

Yujiro Maeoka[1,2], Yan Wu[1], Takumi Okamoto[1], Soshi Kanemoto[1,3], Xiao Peng Guo[1], Atsushi Saito[4], Rie Asada[1,5], Koji Matsuhisa[4], Takao Masaki[2], Kazunori Imaizumi[1*], Masayuki Kaneko[1*]

From the [1]Department of Biochemistry, Institute of Biomedical and Health Sciences, Hiroshima University, 1-2-3 Kasumi, Minami-ku, Hiroshima 734-8553, Japan; [2]Department of Nephrology, Hiroshima University Hospital, 1-2-3 Kasumi, Minami-ku, Hiroshima 734-8551, Japan; [3]Department of Functional Anatomy and Neuroscience, Asahikawa Medical University, 2-1-1-1 Midorigaoka-higashi, Asahikawa, Hokkaido 078-8510, Japan; [4]Department of Stress Protein Processing, Institute of Biomedical and Health Sciences, Hiroshima University, 1-2-3 Kasumi, Minami-ku, Hiroshima 734-8553, Japan; [5]Department of Medicine, Division of Endocrinology, Metabolism, and Lipid Research, Washington University School of Medicine, St. Louis, MO 63110, USA

Running title: *NFAT5 regulates Rnf183 transcription*

[*]To whom correspondence should be addressed: Masayuki Kaneko: Department of Biochemistry, Institute of Biomedical and Health Sciences, Hiroshima University, 1-2-3 Kasumi, Minami-ku, Hiroshima 734-8553, Japan; mkaneko@hiroshima-u.ac.jp; Tel. (81) 82-257-5130; Fax. (81) 82-257-5134

Kazunori Imaizumi: Department of Biochemistry, Institute of Biomedical and Health Sciences, Hiroshima University, 1-2-3 Kasumi, Minami-ku, Hiroshima 734-8553, Japan; imaizumi@hiroshima-u.ac.jp; Tel. (81) 82-257-5130; Fax. (81) 82-257-5134

Keywords: kidney, NFAT transcription factor, promoter, transcription regulation, ubiquitin ligase, RNF183, RNF family, NFAT5, hypertonic stress, renal cell

ABSTRACT

We previously reported that among the 37 RING finger protein (RNF) family members, *RNF183* mRNA is specifically expressed in the kidney under normal conditions. However, the mechanism supporting its kidney-specific expression pattern remains unclear. In this study, we elucidated the mechanism of the transcriptional activation of murine *Rnf183* in inner-medullary collecting duct cells. Experiments with anti-RNF183 antibody revealed that RNF183 is predominantly expressed in the renal medulla. Among the 37 RNF family members, *Rnf183* mRNA expression was specifically increased in hypertonic conditions, a hallmark of the renal medulla. RNF183 up-regulation was consistent with the activation of nuclear factor of activated T cells 5 (NFAT5), a transcription factor essential for adaptation to hypertonic conditions. Accordingly, siRNA-mediated knockdown of NFAT5 down-regulated RNF183 expression. Furthermore, the −3,466 to −3,136-bp region upstream of the mouse *Rnf183* promoter containing the NFAT5-binding motif is conserved among mammals. A luciferase-based reporter vector containing the NFAT5-binding site was activated in response to hypertonic stress, but was inhibited by a mutation at the NFAT5-binding site. ChIP assays revealed that the binding of NFAT5 to this DNA site is enhanced by hypertonic stress. Of note, siRNA-mediated RNF183 knockdown increased hypertonicity-induced caspase-3 activation and decreased viability of mIMCD-3 cells. These results indicate that (i) RNF183 is predominantly expressed in the normal renal medulla, (ii) NFAT5 stimulates transcriptional activation of *Rnf183* by binding to its cognate binding motif in the *Rnf183* promoter, and (iii) RNF183 protects renal medullary cells from hypertonicity-induced apoptosis.

The renal medulla is the only tissue that is constantly under hypertonic conditions to concentrate urine through water reabsorption in mammals (1). The driving forces for water reabsorption are elevated concentrations of sodium chloride and urea, which create exceptionally hypertonic conditions (600 and 2,000 mOsm/kg H_2O under conditions of diuresis and antidiuresis in rodents, respectively) (2). Renal cells, particularly renal medullary cells, partly adapt to the hypertonic conditions by accumulating intracellular organic osmolytes that reduce intracellular ionic strength. Nuclear factor of activated T-cells (NFAT) 5 /tonicity-responsive enhancer binding protein plays a key role in the adaptation to hypertonic conditions by binding to the consensus DNA-binding element RNRNNTTTCCA (where N is any nucleotide, and R is any purine) (3, 4). NFAT5 stimulates the transcription of aldose reductase (AR) (5, 6), sodium- and chloride-dependent betaine transporter (BGT1) (4, 6), sodium myo-inositol co-transporter (SMIT) (3, 6), and heat shock protein 70 (HSP70) (7, 8), which mediate the intracellular accumulation of sorbitol, betaine, and myo-inositol and function as an intracellular molecular chaperone, respectively. In addition to these genes, many downstream genes of NFAT5 are known (9–15). However, a ubiquitin ligase that is directly activated by NFAT5 has not yet been reported.

Ubiquitin ligases are involved in a wide variety of cellular events through ubiquitination (16, 17). RING finger protein (RNF) 183 is a member of the RNF family, which functions as a ubiquitin ligase (18). Previous studies have demonstrated that *RNF183* mRNA expression in the colon of patients with inflammatory bowel disease (IBD) and colorectal cancers was approximately 5- and 2-fold higher than that in control subjects; in these patients, RNF183 promotes intestinal inflammation (19) and proliferation and metastasis of cancers (20), respectively. On the contrary, we previously demonstrated that RNF183 was specifically expressed in human and mouse kidney, and that mouse *Rnf183* mRNA expression in the kidney was approximately 324-fold higher than in the colon (21). To date, however, the reason why *Rnf183* mRNA is selectively expressed in the kidney remains unclear.

In this study, we demonstrated that RNF183 is dominantly expressed in the renal medulla and that NFAT5 regulates *Rnf183* transcription in mouse inner medullary collecting duct (mIMCD-3) cells.

Results

RNF183 is predominantly expressed in the renal medulla

RNF183 has been described as a ubiquitin ligase, which is expressed in normal colonic epithelial cells and colorectal cancer cells (19, 20). In addition, we previously reported that *Rnf183* mRNA expression in the kidney is approximately 324-folds higher than in the colon (21); however, RNF183 protein expression in the kidney remains unclear. To detect RNF183 protein expression, we generated an affinity-purified antibody using recombinant deletion mutant RNF183 (amino acids 61–158) lacking a RING finger domain at its N-terminus and a transmembrane domain at its C-terminus (Figure 1A). The antibody specifically recognized GFP-tagged RNF183 at approximately 50 kDa, which was transiently transfected into human embryonic kidney (HEK) 293 cells (Figure 1B). Immunofluorescence staining using HeLa cells transiently transfected with GFP-RNF183 showed that punctate signals of GFP-RNF183 were recognized by the anti-RNF183 antibody (Figure 1C). GFP signals were localized in the late endosome/lysosome (Lamp1) and early endosome (EEA1), with additional weak signal in the recycling endosome (transferrin receptor, TfR) and Golgi complex (GM130) but not in the endoplasmic reticulum (calnexin) or mitochondria (COX IV) (Figures 1D and S1). To evaluate endogenous RNF183 protein expression, we performed RT-PCR and western blot analysis using tissue extracts in 4-week-old mice. Western blotting revealed that endogenous RNF183 protein was expressed markedly in the kidney, particularly in the renal medulla, and in the thymus (Figure 1, F and H), consistent with *Rnf183* mRNA expression (Figure 1, E and G). Megalin and AR were used as positive controls for the renal cortex and medulla, respectively.

RNF183 expression is up-regulated response to hypertonic stress

Renal medullary cells are constantly exposed to extreme hypertonic stress to concentrate the urine (1). Therefore, using quantitative real-time RT-PCR (qRT-PCR), we

examined whether RNF183 expression and the other transmembrane RNF family members, those containing RING finger (C3H2C3 or C3HC4) and transmembrane domains, are upregulated in response to hypertonic stress. Mouse IMCD-3 cells were incubated with isotonic medium or NaCl- or sucrose-supplemented medium. The extracellular tonicity was increased by approximately 150 mOsm/kg H_2O (final osmolality: 450 mOsm/kg H_2O) by adding 75 mM NaCl or 150 mM sucrose. AR (5, 6) and HSP70 (7, 8) were used as positive controls for tonicity dependence. We found that *Rnf183* mRNA expression was markedly upregulated in a tonicity-dependent manner in both hypertonic NaCl- and sucrose-treated cells compared with that in isotonic control cells (Figure 2A), which was consistent with the AR and HSP70 upregulation patterns (Figure 2A). *Rnf128* and *Rnf19B* were modestly upregulated in a tonicity-dependent manner. Further, *Rnf24*, *Rnf13*, *Rnf167*, *Rnf43*, *Syvn1*, *Amfr*, *Rnf145*, *Rnf5*, *Rnf185*, and *Rnf170* were slightly upregulated in cells treated with only 75 mM NaCl; the other RNF family members were not upregulated (Figure 2A). Western blot analysis showed that RNF183 and AR protein expression was upregulated in a tonicity-dependent manner (Figure 2, B–E). However, *Rnf183* mRNA was not upregulated under hypoxic conditions (oxygen concentration, 1% and 0.3%) (Figure S2), which is another characteristic of the renal medulla. These results suggest that hypertonic conditions play a more important role in RNF183 expression than hypoxic conditions. Next, we examined whether RNF183 upregulation was different between mIMCD-3 cells and other renal cell lines. Normal rat kidney (NRK)-52E (a rat kidney tubular epithelial cell line), NRK-49F (a rat kidney interstitial fibroblast cell line), mIMCD-3, and HEK 293 cells were used. HEK 293 cells transiently transfected with mouse RNF183 were used as a positive control. We found that RNF183 expression increased markedly in mIMCD-3 cells treated with hypertonic NaCl and increased slightly in NRK-52E cells, whereas no expression was detected in NRK-49F and HEK293 cells (Figure 2F). Interestingly, the difference in RNF183 expression among renal cell lines was similar to that in AR expression. The similarity between RNF183 and AR upregulation in response to hypertonic stress suggests that NFAT5 regulates RNF183 expression as well as AR expression.

RNF183 expression is upregulated concurrently with NFAT5 activation

The NFAT5 transcription factor is the master regulator for hypertonic stress in mammals (22). In response to hypertonic stress, NFAT5 activation is achieved by a combination of NFAT5 induction and localization into the nucleus (4, 23, 24). Thus, we evaluated the effects of hypertonicity on NFAT5 activation in mIMCD-3 cells. We performed immunofluorescence staining of NFAT5 and plotted the fluorescence intensity along a line drawn through the nucleus. These analyses showed that NFAT5 was present in both the cytoplasm and nucleus under isotonic conditions (Figure 3A). Hypertonic stimulation for 3 h reduced NFAT5 cytoplasmic expression and slightly enhanced nuclear expression, and that for 12 h drastically enhanced nuclear expression

(Figure 3A). Western blot analysis demonstrated that the total abundance of NFAT5 protein significantly increased after 3 h of hypertonic stimulation and peaked at 9 h (Figure 3, B and C), consistent with NFAT5 localization (Figure 3A). Moreover, qRT-PCR analysis revealed that the expression of *Rnf183* and NFAT5 downstream genes, AR (5, 6) and HSP70 (7, 8), concurrently increased after 3 h of hypertonic stimulation (Figure 3D). The RNF183 and AR protein levels significantly increased after 6 and 9 h of hypertonic stimulation (Figure 3, E and F), respectively. In contrast to the downstream genes of NFAT5, the TNF-α mRNA level, which is that of NF-κB, peaked after 3 h of hypertonic stimulation and decreased after 6 h (Figure S3). These results demonstrated that RNF183 expression was upregulated under hypertonic conditions and was accompanied by NFAT5 activation and the upregulation of NFAT5 downstream genes, suggesting that RNF183 expression is directly mediated by NFAT5.

NFAT5 knockdown and p38/MAPK inhibitor SB203580 attenuate hypertonicity-induced RNF183 expression

To determine the effect of NFAT5 inhibition on RNF183 expression, mIMCD-3 cells were transfected with siRNA oligonucleotides targeting NFAT5 (NFAT5 siRNA #1) or negative control siRNA (NC siRNA). After 12 h of hypertonic stimulation, the NFAT5 protein levels were significantly reduced in mIMCD-3 cells transfected with NFAT5 siRNA #1 (Figure 4, A and B). NFAT5 knockdown significantly inhibited the hypertonicity-induced RNF183 protein and mRNA expression of both *Rnf183* and AR (Figure 4, C–E). Another NFAT5 siRNA (NFAT5 siRNA #2) produced similar results (Figure S4, A–C). The hypertonic stress signal is mediated through p38/MAPK, which regulates NFAT5 activation in mammals [12, 13, 25, 26]. Thus, to determine the effect of p38/MAPK inhibition on RNF183 expression, mIMCD-3 cells were treated with 75 mM NaCl-supplemented medium in the presence of the indicated concentration of SB203580. The hypertonicity-induced protein and mRNA expression of RNF183 and NFAT5 downstream genes AR and SGK1 were concurrently inhibited by SB203580 in a dose-dependent manner (Figure 4, F and G). These results demonstrated that RNF183 expression depends on NFAT5.

Identification of the Rnf183 enhancer region that responds to hypertonic stress

To identify the putative enhancer region in the *Rnf183* promoter, we searched for an evolutionary conserved region (ECR) within 5,000 base pair (bp) upstream of the human *RNF183* gene using the ECR browser (27). The 319-bp region (−4,367 to −4,049 region; numbers indicate nucleotide positions relative to the transcription start site) upstream of the human *RNF183* gene was identified to be conserved in mammals (blue; Figure 5A). Although its actual position from the transcription start site varies among the species (Figure 5B), it shows high sequence identity with the corresponding region in the following mammals: *Mus musculus*, 71%; *Rattus novegicus*, 73%; *Canis familiaris*, 81%; *Bos taurus*, 80%; *Macaca mulatta*, 94%; and *Pan troglodytes*, 98%. We next searched for potential binding sites for various transcription factors

within the mammalian conserved region of *RNF183* genes (−3,466 to −3,136, mouse, left; −1,978 to −1,664, rat, upper right; −4,367 to −4,049, human, lower right) using the JASPAR database (28). This analysis identified one binding site for NFAT proteins conserved among mouse, rat, and human (Tables 1 and S1). The sequences (GTACTTTTCCA: −3,342 to −3,332; numbers indicate the nucleotide position relative to the transcription start site of mouse *Rnf183*, GTACTTTTCCA: −1,870 to −1,860; those of rat *RNF183*, GTGCTTTTCCA: −4,256 to −4,246; those of human *RNF183*) were completely homologous with the NFAT5 consensus sequence (RNRNNTTTCCA) (3, 4) (Figure 5B). Furthermore, the sequences around the binding site were highly conserved among mouse, rat, and human (blue background). Between the conserved region and the transcription start site of mouse *Rnf183* gene (−3,135 to −1), we found another site (AGGTTTTTCCA: −538 to −528) that was completely homologous with the NFAT5 consensus sequence, but not conserved among the species. To determine whether NFAT5 acts on the *Rnf183* promoter containing these sites to activate *Rnf183* transcription, we performed luciferase reporter assays using the promoter region in mIMCD-3 cells. A 3.5-kbp (containing both NFAT5 DNA binding sites) or 2.0-kbp (containing non-conserved NFAT5 DNA binding site) promoter regions of the mouse *Rnf183* gene (pGL4-3.5 kbp-Luc and pGL4-2.0 kbp-Luc, respectively; Figure 5C) were used. The reporter activity of pGL4-3.5 kbp-Luc, but not that of pGL4-2.0 kbp-Luc or pGL4-Luc, was considerably induced by hypertonic stress (Figure 5D). These results demonstrated that the putative *Rnf183* enhancer region has responsiveness to hypertonic conditions.

***Rnf183* enhancer region depends on NFAT5**

To determine whether the putative *Rnf183* enhancer region was dependent on NFAT5, we examined the effects of NFAT5 knockdown, p38/MAPK inhibition, and the dominant negative (DN) form of NFAT5 on luciferase activities. NFAT5 knockdown markedly reduced the reporter activity of pGL4-3.5 kbp-Luc (Figures 6A and S4D), whereas FLAG-NFAT5 overexpression fully rescued the downregulated reporter activity (Figures 6B and S5). p38/MAPK inhibitor SB203580 significantly inhibited the hypertonicity-induced *Rnf183* luciferase activities (Figure 6C), which is consistent with mRNA and protein expression of RNF183 (Figure 4, F and G). Moreover, *Rnf183* luciferase activities were inhibited by overexpression of DN-NFAT5, whereas they were upregulated by that of the full-length NFAT5 (Figure 6D). These results suggest that the putative *Rnf183* enhancer region depends on NFAT5.

***Rnf183* is a direct target of NFAT5**

We next performed luciferase reporter assays using pGL4-3.5 kbp-Luc of WT and mutant having a mutation in the conserved NFAT5 DNA binding site (Figure 7A). In mIMCD-3 cells transfected with the mutant, reporter activities were markedly reduced even in hypertonic conditions (Figure 7B). Consistent with this, NFAT5 overexpression markedly induced WT reporter activity of WT, which was inhibited by the mutation (Figure 7C). To confirm whether NFAT5 directly binds to the

conserved binding site in the *Rnf183* promoter, we performed ChIP assays using mIMCD-3 cells under hypertonic conditions (Figure 7D) and detected a high level of NFAT5 binding to the conserved binding site in the endogenous *Rnf183* promoter (Figure 7, E and F). These results indicated that NFAT5 directly acts on the conserved NFAT5 DNA binding site within the *Rnf183* promoter and facilitates its transcription in mIMCD-3 cells.

RNF183 expression provides protection against hypertonicity-induced apoptosis

Stress induced by an elevated NaCl concentration mediated apoptosis in mIMCD3 cells when osmolality is acutely raised to >600 mOsm/kg (29–31). Moreover, several NFAT5 downstream genes show a protective effect against hypertonicity-induced apoptosis (9, 32, 33). Thus, to determine whether RNF183 expression affects the osmotic tolerance of mIMCD-3 cells to high NaCl levels, mIMCD-3 cells were transfected with siRNA oligonucleotides targeting RNF183 (RNF183 siRNA) or NC siRNA. RNF183 siRNA effectively reduced the *Rnf183* mRNA levels compared with NC siRNA (Figure 8A). After 4 h of exposure to 200 mM NaCl-supplemented media, cleaved caspase-3 protein levels and cleaved caspase-3-positive cells (which are indexes of apoptosis) significantly increased in mIMCD-3 cells transfected with RNF183 siRNA (Figure 8, B and C). Crystal violet assays revealed that RNF183 knockdown significantly reduces cell viability under hypertonic conditions (Figure 8D). In contrast, RNF183 knockdown did not promote caspase activation upon treatment of mIMCD-3 cells with the apoptosis inducer staurosporine (Figure S6). These results demonstrate that RNF183 protects inner-medullary cells from hypertonicity-induced apoptosis.

Rescue of RNF183 knockdown attenuates hypertonicity-induced apoptosis

To eliminate the possibility of siRNA off-target effects, mIMCD-3 cells transfected with RNF183 siRNA or NC siRNA were rescued with siRNA-resistant 3×FLAG-RNF183, which was expressed in mIMCD-3 cells under RNF183 knockdown (Figure 9A). After 4 h of exposure to 200 mM NaCl-supplemented media, cleaved caspase-3 protein levels significantly decreased in mIMCD-3 cells rescued with 3×FLAG-RNF183 (Figure 9B). Crystal violet assays showed that the rescue of RNF183 knockdown significantly improved cell viability under hypertonic conditions (Figure 9C). These results confirm that RNF183 protects inner-medullary cells from hypertonicity-induced apoptosis.

Discussion

We identified the conserved NFAT5 DNA binding site in the *Rnf183* enhancer region and found that this site induced RFN183 reporter activity under hypertonic conditions, whereas mutation at the site resulted in almost complete inhibition of *Rnf183* reporter activity. In addition, ChIP assays revealed a high level of NFAT5 binding to the site. Thus, these results demonstrated a mechanism of RNF183 upregulation under hypertonic conditions by which NFAT5 directly binds to the conserved NFAT5 DNA binding site in the *Rnf183* enhancer region and leads to its transcriptional

activation. This is the first study to demonstrate that ubiquitin ligase can be directly regulated by NFAT5. However, Yu et al. demonstrated that microRNA-7 (miR-7) directly bound to the 3′-UTR of *RNF183* mRNA leading to *RNF183* degradation and translational inhibition, and that downregulation of miR-7 induced RNF183 elevation in inflamed colon tissues of IBD patients and colitic mice (19). Of the two regulators of RNF183 expression, we considered NFAT5 to be more important than miR-7 in a normal kidney because the tissue distribution pattern of RNF183 is different from that of miR-7 (34). The expression of miR-7 is restricted to specific tissues of the brain, colon, and thymus, whereas it is extremely low in the kidney, heart, liver, lung, spleen, and stomach (34), which is not consistent with our results on RNF183 expression (Figure 1, E and F). While NFAT5 is broadly expressed as an essential factor during exposure to the hypertonic environment (4), systemic or immature thymocyte-specific NFAT5 knockout mice display profound defects in the renal medulla and reduced thymocyte compartment in the thymus, respectively (6, 35, 36). This is because NFAT5 is activated by hypertonicity-dependent and -independent pathways in the renal medulla (6, 37, 38) and thymus (36), respectively. Consistent with these findings, RNF183 was highly expressed in the renal medulla and was also expressed in the thymus (Figure 1, E–H). Therefore, we hypothesized a mechanism by which high RNF183 expression in the normal kidney and thymus is predominantly regulated by the NFAT5 activation, but not miR-7.

We observed an approximately 2- to 3-fold increase in the induction of *Rnf183* reporter activity following hypertonic stimulation. One possible explanation for this mild induction of the *Rnf183* promoter is that only a short sequence of the *Rnf183* promoter was investigated. Consistent with our results, Hasler *et al.* and Chen *et al.* have demonstrated that the activity of AQP2 and SGK1 promoters (each containing one NFAT5 binding element) increased approximately 1.5- and 5-fold, respectively, following hypertonic stimulation (12, 39). However, at least five NFAT5 binding elements spread over 50-kb pairs, which participate in NFAT5-mediated transcriptional stimulation, were revealed in the SMIT promoter (3). Similarly, three NFAT5 binding sequences that were identified in the AR promoter may collectively participate in the hyperosmotic response (5). Therefore, other NFAT5 binding elements may be present in regions of the *Rnf183* promoter that are further upstream or downstream. Moreover, we demonstrated that *Rnf183* reporter activity and *Rnf183* and AR mRNA expression were concurrently reduced by NFAT5 knockdown under isotonic conditions. Several previous studies have shown that, to some extent, NFAT5 knockdown or dominant negative NFAT5 expression inhibited mRNA expression or promotor activity of its downstream genes under isotonic conditions (7, 9, 39, 40). In contrast, two studies have shown that NFAT5 inhibition did not affect the basal expression of its downstream genes under isotonic conditions (12, 41). This difference in NFAT5 inhibition may result from variation in the basal NFAT5 protein levels because basal AR protein expression levels were high in mIMCD-3 cells compared with those in other renal cell lines (Figure 2F).

We further examined whether RNF183 was upregulated by hypoxia in mIMCD-3 cells because the renal medulla is characteristically hypoxic (42). Although vascular endothelial growth factor A (VEGFA) mRNA, which is downstream of the hypoxic master regulator hypoxia-inducible factor 1 (HIF-1) (43), was significantly upregulated under hypoxia (oxygen concentration: 1% and 0.3%), *Rnf183* was not upregulated (Figure S2). Moreover, HIF-1 DNA binding site (ACGTG) was not observed in the *Rnf183* enhancer region (Table S1). These results suggest that the high RNF183 expression in the renal medulla dose not result from hypoxia.

Our results demonstrated that *Rnf183* mRNA was markedly up-regulated compared with the other transmembrane RNF family members under hypertonic conditions, and that the siRNA-induced knockdown of RNF183 exacerbates apoptosis and reduces cell viability in mIMCD-3 cells at approximately 700 mOsm/kg. Although the effects of RNF183 on adaptation to hypertonicity appear to be mild, we consider RNF183 to be as important as other NFAT5 regulated genes. Lee *et al.* demonstrated up to a 1.5-fold increase in the hypertonicity-induced LDH release in MEF cells transfected with siRNA targeting SMIT, BGT1, AR, or HSP70, etc. [44]. Shim *et al.* have also demonstrated an approximately 20% to 30% decrease in cell viability following 100-mM NaCl supplementation in HSP70-knockout MEF cells [33]. Their effects on adaptation to hypertonicity appear to be similar to that of RNF183 in the present study. Therefore, RNF183 expression is induced by hypertonic stress and plays an important role in the kidney's osmoprotective function under hypertonic conditions. However, we could not clarify the substrate of RNF183 under hypertonic conditions. To date, three previous studies have demonstrated the different functions of RNF183 in cancers and the colon as follows: 1) In tumors, RNF183 interacts with fetal and adult testis expressed 1 (FATE1), which is a cancer/testis antigen, and negatively regulates the apoptotic effector Bcl-2-interacting killer (BIK), a component of FATE1 complex, leading to increased tumor cell viability (45), 2) In the colon, RNF183 degrades IκBα, thereby inducing NF-κB activation, which might contribute the pathogenesis of IBD (19), 3) In the colorectal cancers, RNF183 induces the activation of NF-κB and expression of its downstream gene, IL-8, resulting in increased proliferation and metastasis of colorectal cancer cells (20). However, FATE1 expression is restricted to cancer or testis and is absent in the other tissues, such as the kidney (45). Moreover, NF-κB activation by hypertonicity is transient and starts decreasing after 3h of hypertonic stimulation in cortical collecting duct cells due to the restoration of IκBα protein levels (46, 47). Consistent with this, the mRNA level of TNF-α, a NF-κB downstream gene, peaked after 3 h of hypertonic stimulation and decreased after 6 h at the time of RNF183 protein level elevation (Figure S3). Hence, these results suggest that RNF183 ubiquitylates other substrates under hypertonic conditions as there is a contradiction on whether the NFAT5–RNF183 axis regulates BIK and IκBα expression.

RNF183 expression in response to hypertonicity is mediated by NFAT5, which is essential for long-term adaptation to hypertonic

conditions (48). Short-term adaptation involves rapid influx of electrolytes and amino acids through various transporters, such as Na^+-K^+-Cl^- cotransporters, Na^+/H^+ exchangers, Cl^-/HCO_3^- exchangers (49), and sodium-coupled neutral amino acid transporter 2 (50). Long-term adaptation involves delayed replacement of ionic osmolytes with uncharged small organic osmolytes via expression of various enzyme and transporters, such as AR (5, 6), BGT1 (4, 6), and SMIT (3, 6), mediated by NFAT5. However, in long-term adaptation, the mechanism by which the dispensable transporters of ionic osmolytes are downregulated remains unclear. Here, the punctate signals of RNF183 were predominantly localized to endosomes and lysosomes (Figure 1D). Early or late endosome-localized ubiquitin ligases can sort internalized cell-surface receptors from the recycling pathway to lysosomal degradation through ubiquitination (51–53). Therefore, we speculated that RNF183 plays a role in sorting internalized dispensable transporters to lysosomes for long-term adaptation to hypertonic conditions.

In summary, NFAT5 directly binds to the conserved DNA binding site in the *Rnf183* enhancer region and leads to *Rnf183* transcriptional activation, thereby inducing its high expression in the renal medulla. Among the transmembrane RNF family members, *Rnf183* is specifically upregulated by hypertonic stress and protects the cells from hypertonicity-induced apoptosis. However, our study did not include identification of substrate for RNF183 and validation by animal experiments under hypertonic conditions. Further study is warranted to elucidate the localization and function of RNF183 in the kidney.

Experimental procedures

Plasmids

A full-length mouse RNF183 construct with a stop codon was transferred from pENTR/D-TOPO (cat# 45-0218, Invitrogen, CA) (54) into the Vivid Colors pcDNA6.2/N-EmGFP-DEST vector (cat# 35-1017, Invitrogen) containing a N-terminal emerald GFP and into pcDNA6.2-DEST (cat# 35-1264, Invitrogen) using Gateway LR Clonase II Enzyme mix (cat# 12538-120, Invitrogen). The 3×FLAG-RNF183 construct synthesized using GeneArt Strings DNA Fragments (Invitrogen) was cloned into the pENTR/D-TOPO (Invitrogen). The entry clone product was recombined into the pcDNA6.2-DEST vector using LR Clonase II Enzyme mix. The deletion mutant mouse RNF183 (amino acids 61–158) with a stop codon was amplified by PCR using the following primer sets and was subcloned into pENTR/D-TOPO:
5′-CACCATGCAGCCCACCGT-3′ (forward) and
5′-TCAGAAGTGAGGGTTGCGGACACA-3′ (reverse). Subsequently, using Gateway LR Clonase II Enzyme mix, the sequence was transferred into the pDest-565 vector (cat# 11520, Addgene, MA), containing a glutathione *S*-transferase (GST) at the N-terminus of insert sequences and into the pDest-566 vector (cat# 11517, Addgene) containing a maltose-binding protein (MBP) at the N-terminus of insert sequences. pFLAG-NFAT5, the expression vector of NFAT5, was gifted to us by Dr. B. C. Ko (23) and Dr. Takashi Ito (9). The pFLAG-DN-NFAT5 was a generous gift from

Dr. Takashi Ito (9).

Rnf183 promoter fragments were amplified from C57BL/6 murine genomic DNA by PCR using the following primer sets: 3,525 bp (−3465 to +60 region; numbers indicate the nucleotide position relative to the transcription start site), 5′-GGTACCTTTCCCAGAAAGCCCATCCC-3′ (forward) and 5′-TTTCTCGAGTGTGAGTCACCCCTGCTTTC-3′ (reverse); 2,012 bp (−1,952 to +60 region), 5′-CTGGTACCTCAAGAGCCATTGAAAGAACACT-3′ (forward) and 5′-TTTCTCGAGTGTGAGTCACCCCTGCTTTC-3′ (reverse). Subsequently, the purified products were subcloned into the pGL4.10[*luc2*] vector (cat# 9PIE665, Promega, WI) between *KpnI* and *XhoI* sites, respectively. The resulting vectors were named pGL4-3.5 kbp-Luc and pGL4-2.0 kbp-Luc, respectively. Mutagenesis of the conserved NFAT5 DNA-binding site (−3,358 GTACTGCTTAGGCCAGGTACTTTTCCAGCTGGCTGGCCTGC; NFAT5 DNA binding site is underlined) was performed using the QuickChange Lightning site-directed mutagenesis kit (cat# #210518, Agilent Technologies, CA) and the following series of oligonucleotides (sequence represents anti-sense strand, with mutagenized bases represented in lower case): M1, −3,358 GTACTGCTTAGGCCAGGTcCTTaTCaAGCTGGCTGGCCTGC; M2, −3,358 GTACTGCTTAGGCCAGGaACTTTTttAGCTGGCTGGCCTGC.

Antibodies

For obtaining the recombinant deletion mutant, plasmids containing RNF183 (amino acids 61–158) fused to GST (pDEST-565) or MBP (pDEST-566) were transformed into the *Escherichia coli* strain BL21 (DE3) (cat# 69450-3, Millipore, Tokyo, Japan); protein expression was induced by isopropyl β-d-1-thiogalactopyranoside (cat# R0392, Thermo Fisher Scientific, MA). Rabbit antiserum was raised against the GST-tagged protein, and affinity purification was performed using a HiTrap NHS-activated HP column (cat# 17-0716-01, GE Healthcare, UK) coupled with MBP-tagged protein.

Animals

Four-week-old C57BL/6 mice were used in this study. All animal experiments were performed in accordance with the NIH Guidelines for the care and use of laboratory animals and were approved by the Committee of Animal Experimentation, Hiroshima University. The mice were maintained in a room at 23°C and a constant day–night cycle and were provided food and water ad libitum.

Cell culture, treatments, and transfection

HEK293, HeLa, mIMCD-3, NRK-49F, and NRK-52E cells were maintained in Dulbecco's Modified Eagle's Medium (DMEM; cat# 12800-017, Gibco, NY) or DMEM/Nutrient Mixture F-12 (DMEM/F-12, cat# 12500-062, Gibco) supplemented with 10% (v/v) heat-inactivated fetal bovine serum at 37°C in a 5% CO_2 and 95% humidified air atmosphere. To induce hyperosmotic stress, cells received equal volumes of DMEM/F-12 (control) or 75 mM NaCl or 150 mM sucrose in DMEM/F-12 for the indicated time, according to the method reported

by Bell *et al.* (55). For knockdown experiments, mIMCD-3 cells were transfected with three types of NFAT5-targeting Silencer siRNA (cat# 4390771 ID: s21069 and s203948, cat# 4399665 ID: s550857, Invitrogen) or a RNF183-targeting Silencer siRNA (cat# 4390771 ID: s94062, Invitrogen) or a negative control Silencer siRNA (cat# 4390843, Invitrogen) as a control using ScreenFect siRNA (cat# 295-75003, Wako Pure Chemical Industries, Osaka, Japan) in 6-well plates (12.5 pmol/well). HeLa or HEK293 cells were transfected with each expression plasmid using ScreenFect A (cat# 297-73204, Wako Pure Chemical Industries). For inhibition of p38/MAPK, mIMCD-3 cells were preincubated with SB203580 at 0–25 μM (cat# 199-16551, Wako Pure Chemical Industries) for 1 h and treated with 75-mM NaCl-supplemented medium for the indicated time, according to the method reported by Chen *et al.* (12).

Analysis of mRNA levels in murine tissues

Total murine tissue RNA was extracted from C57BL/6 mice using ISOGEN (cat# 311-02501, Nippon Gene, Toyama, Japan) according to the manufacturer's protocol. Reverse transcription was performed with ReverTra Ace (cat# TRT-101, Toyobo Co., Ltd., Osaka, Japan). PCR was performed using the following primer sets in a total volume of 20 μL containing 0.2 μM of each primer, 0.2 mM dNTPs, 1 unit of Paq5000 DNA polymerase, and 10× PCR buffer (cat# 600680, Agilent Technologies): mouse *Rnf183*, 5′-GACCAGCCCAAGAGCCGCTA-3′ (forward) and 5′-CCCCAAAAGAACTGCTTAGTCCA-3′ (reverse); mouse Megalin, 5′-CTCCTGCAAGTCGGTCCATT-3′ (forward) and 5′-GACCGCCCAGTAGAGCTTTT-3′ (reverse); mouse AR, 5′-AGAGCATGGTGAAAGGAGCC-3′ (forward) and 5′-TGGCACTCGATCTGGTTCAC-3′ (reverse). The PCR conditions were as follows: 94°C for 2 min, 22–26 cycles at 98°C for 10 s, 60°C for 30 s, 72 °C for 30 s, and 72°C for 3 min. The PCR products were resolved by electrophoresis on a 4.8% acrylamide gel. The density of each band was quantified using the Adobe Photoshop Elements 2.0 program (Adobe Systems Inc.).

Analysis of mRNA levels in culture cells

Total RNA from mIMCD-3 cells was extracted using ISOGEN. Reverse transcription was performed with ReverTra Ace (cat# TRT-101, Toyobo Co., Ltd.). The reverse-transcribed cDNA was measured by TaqMan-based real-time PCR assay using the ΔΔ Ct method. The following TaqMan primer and probe sets, purchased from Integrated DNA Technologies (Coralville, IA) were used: mouse *Rnf183* (assay ID: Mm.PT.58.42013627), mouse AR (assay ID: 214320988), mouse HSP70 (assay ID: Mm.PT.58.31570020.g), mouse VEGFA (assay ID: Mm.PT.58.31754187), mouse TNFα (assay ID: Mm.PT.58.29509614), mouse *Rnf130* (assay ID: Mm.PT.58.9219868), mouse *Rnf150* (assay ID: Mm.PT.58.10273312), mouse *Rnf149* (assay ID: Mm.PT.58.11306683), mouse *Rnf133* (assay ID: Mm.PT.58.43776563.g), mouse *Rnf128* (assay ID: Mm.PT.56a.8462982), mouse *Rnf122* (assay ID: Mm.PT.58.8505793), mouse *Rnf24* (assay ID: Mm.PT.58.9635653), mouse *Rnf13* (assay ID: Mm.PT.58.11306683), mouse *Rnf167* (assay

ID: Mm.PT.58.32670381), mouse *Znf4* (assay ID: Mm.PT.58.32478833.g), mouse *Rnf43* (assay ID: Mm.PT.56a.31556976), mouse *Znf3* (assay ID: Mm.PT.56a.5645486), mouse *Syvn1* (assay ID: Mm.PT.58.14132695), mouse *Amfr* (assay ID: Mm.PT.58.9856954), mouse *Rnf121* (assay ID: Mm.PT.58.6378114), mouse *Rnf145* (assay ID: Mm.PT.58.10110397), mouse *Rnf139* (assay ID: Mm.PT.58.45812642), mouse *Rnf103* (assay ID: Mm.PT.58.9763784), mouse *Rnf19A* (assay ID: Mm.PT.58.28600163), mouse *Rnf19B* (assay ID: Mm.PT.58.28736280), mouse *Rnf5* (assay ID: Mm.PT.58.14209781), mouse *Rnf185* (assay ID: Mm.PT.56a.11642500), mouse *Rnf170* (assay ID: Mm.PT.56a.13272002), mouse *Rnf186* (assay ID: Mm.PT.56a.29338718.g), mouse *Rnf152* (assay ID: Mm.PT.58.29277956.g), mouse *Rnf182* (assay ID: Mm.PT.58.30902864.g), mouse *Trim59* (assay ID: Mm.PT.58.30417218), mouse *Trim13* (assay ID: Mm.PT.56a.9751937), mouse *Bfar* (assay ID: Mm.PT.56a.28494992), mouse *Rnf180* (assay ID: Mm.PT.58.45835696), mouse *Rnft1* (assay ID: Mm.PT.58.6836835), mouse *Rnf26* (assay ID: Mm.PT.58.5764306.g), mouse *Cgrnf1* (assay ID: Mm.PT.58.5664724), mouse *Mul1* (assay ID: Mm.PT.58.11670267), and mouse *Rnf217* (assay ID: Mm.PT.56a.33323466). Mouse β-actin TaqMan primer and probe set was as follows: 5′-GCGGTTCCGATGCCCT-3′ (forward), 5′-CATGGATGCCACAGGATTCC-3′ (reverse), and 5′-AGGCTCTTTTCCAGCCTTCCTTCTTGG-3′ (probe).

Western blotting

Tissue or cell lysates were prepared in 1× Laemmli sample buffer. Equivalent protein samples were loaded onto SDS-polyacrylamide gels. Gels were transferred to Immobilon-P PVDF membranes (cat# IPVH00010, Millipore) and blocked in 5% non-fat dry milk at room temperature for 1 h. The membrane was incubated with primary antibody at 4°C overnight and with secondary antibody at room temperature for 1h. The following primary antibodies were used: anti-β-actin (cat# sc47778, Santa Cruz Biotechnology, CA), anti-Aldose reductase (cat# sc271007, Santa Cruz Biotechnology), anti-cleaved caspase-3 (cat# 9661, Cell Signaling Technology, MA), anti-GFP (cat# 598, Medical Biological Laboratories, Nagoya, Japan), anti-Megalin (cat# 101-M144, ReliaTech GmbH, Germany), anti-NFAT5 (cat# ab3446, Abcam, UK), and anti-RNF183. The secondary antibodies used were as follows: horseradish peroxidase (HRP)-conjugated goat anti-mouse immunoglobulin G antibody (cat# 1031-05 Southern Biotech, AL) and HRP-conjugated goat anti-rabbit antibodies (cat# 4050-05 Southern Biotech). Images were obtained using WSE-6100 LuminoGraph (ATTO Corporation, Tokyo, Japan).

Immunofluorescence

Cells were fixed in 4% paraformaldehyde at room temperature for 10min and then permeabilized in methanol at −20°C for 10min. Cells were blocked with 5% anti-goat serum at room temperature for 30 min and incubated with primary antibody at 4°C overnight and then with Alexa Fluor-conjugated secondary antibodies at room temperature for 30 min. The following primary antibodies were

used: anti- GFP (cat# 598, Medical Biological Laboratories), anti-NFAT5 (cat# ab3446, Abcam), anti-cleaved caspase-3 (cat# 9661, Cell Signaling Technology), anti-Calnexin (cat# 2679, Cell Signaling Technology), anti-COX IV (cat# 4850, Cell Signaling Technology), anti-EEA1 (cat# 3288, Cell Signaling Technology), anti-GM130 (cat# 12480, Cell Signaling Technology), anti-Transferrin Receptor (cat# 13-6800, Invitrogen), and anti-Lamp1 (cat# 9091, Cell Signaling Technology). The secondary antibodies used were as follows: goat anti-mouse AlexaFluor555 (cat# A-21422, Invitrogen), goat anti-rabbit AlexaFluor568 (cat# A-11036, Invitrogen), goat anti-mouse AlexaFluor488 (cat# A-11001, Invitrogen), and goat anti-rabbit AlexaFluor488 (cat# A-11070, Invitrogen). ProLong Diamond Antifade Mountant with DAPI (cat# P36962, Invitrogen) was used to mount slips on glass slides. Fluorescence images were acquired using an Olympus FluoView FV1000 confocal microscope (Olympus, Tokyo, Japan). Apoptotic cells were counted in five different fields of view and the ratio of the number of cleaved caspase 3-positive cells to that of DAPI-stained cells was calculated.

Luciferase assay

Mouse IMCD-3 cells were transiently transfected with 0.2 μg of pGL4.10[*luc2*] carrying both the firefly luciferase gene and the referenced constructs and 0.02 μg of pGL4.74[hRluc/TK] carrying the *Renilla* luciferase gene under the control of the herpes simplex virus thymidine kinase enhancer and promoter (cat# 9PIE692, Promega) in the presence of NFAT5 siRNA #1, NFAT5 siRNA #2 (cat# 4390771, Invitrogen), NFAT5 siRNA #3 (cat# 4399665, Invitrogen), NC siRNA (cat# 4390843, Invitrogen), empty, pFLAG-DN-NFAT5, or pFLAG-NFAT5 vectors; the transfection was performed using ScreenFect A (cat# 297-73204, Wako Pure Chemical Industries) under conditions recommended by the manufacturer. For rescue of NFAT5 knockdown, cells pre-transfected with siRNA (NFAT5 #3 or NC) using ScreenFect siRNA (cat# 295-75003, Wako Pure Chemical Industries) were cotransfected with 3.5 kbp-Luc and either empty or pFLAG-NFAT5 vectors after 12 h of knockdown. Twenty-four hours after transfection, cells were treated with 75 mM NaCl or 150 mM sucrose in DMEM-F12 for 24 h. Cells were washed twice with phosphate-buffered saline (PBS) and subsequently lysed with Passive Lysis Buffer (cat# 194A, Promega). Luciferase activities were measured with Dual-Luciferase Reporter Assay System (cat# 1960, Promega) and a GloMax Multi+ Detection System (Promega), according to the manufacturer's protocol. Relative activity was defined as a ratio between activities of firefly luciferase and *Renilla* luciferase. The vector pGL4.10[*luc2*] without the promoter (pGL4-Luc) was used as a negative control.

ChIP Assay

Two 10-cm plates of approximately 80% confluent mIMCD-3cells were cultured for 24 h and treated with 75 mM NaCl for 4 h prior to cross-linking. Cells were treated with 1% (v/v) formaldehyde for 15 min at 37 °C, followed by an additional 5 min in 150 mM glycine. Subsequently, cells were washed with cold PBS and lysed in nuclear lysis buffer [50 mM Tris-HCl (pH 8.0), 10 mM EDTA, 1% SDS, and

protease inhibitor cocktail] for 10 min on ice. Nuclear lysates were sonicated to a final average fragment length of 1,000 bp using a Bioruptor II (BM Equipment, Tokyo, Japan). Sonicated chromatin was cleared by centrifugation at 13,000 *rpm* for 10 min and then diluted 10-fold with dilution buffer [16.7 mM Tris-HCl (pH8.0), 1.2 mM EDTA, 0.01% SDS, 1.1% Triton X-100, 167 mM NaCl, and protease inhibitor cocktail]. The soluble chromatin was incubated with 2 μg of normal IgG rabbit (cat# 2729, Cell Signaling Technology) or anti-NFAT5 antibody (cat# ab3446, Abcam) on a rotating platform at 4°C overnight, followed by incubation with 20 μL of Magna ChIP Protein A+G magnetic beads (cat# 16-663, Millipore) for 1 h. Subsequently, the beads were washed with the following four buffers: low salt buffer [20 mM Tris-HCl (pH 8.0), 2 mM EDTA, 0.1% SDS, 1% Triton X-100, 150 mM NaCl], high salt buffer (same as low salt buffer with 500 mM NaCl), LiCl buffer [10 mM Tris-HCl (pH 8.0), 1 mM EDTA, 0.25 M LiCl, 1% NP-40, 1% sodium deoxycholate], and TE buffer [10 mM Tris-HCl (pH 8.0), 1 mM EDTA]. Precipitated complexes were eluted twice from the beads in fresh elution buffer (1% SDS, 0.1 M $NaHCO_3$) for 30 min each at room temperature and subsequently heated at 65°C overnight to reverse formaldehyde-induced cross-linking. The DNA was purified by phenol–chloroform extraction and ethanol precipitation. The purified DNA was amplified by PCR in a total volume of 20 μL containing 0.45 μM of each primer, 0.4 mM dNTPs, 1 unit of KOD FX DNA polymerase, and 2× PCR buffer (cat# KFX-101, Toyobo). The following primer set was used, yielding a 303-bp product: 5′-GTTTTACCCTTTTGCCTGTTTCCTT-3′ (forward) and 5′-CAGGCTAAGAAGTCCTTGGTAAACA-3′ (reverse). The PCR conditions were as follows: 94°C for 5 min, 33 cycles at 94°C for 15 s, 60°C for 30 s, 68°C for 20 s, and 68°C for 3 min. The PCR products were resolved by electrophoresis on a 4.8% acrylamide gel. The density of each band was quantified using the Adobe Photoshop Elements 2.0 program (Adobe Systems Inc.).

Cell viability assay

mIMCD-3 cells were transfected with RNF183 or NC siRNA in 6-well plates (12.5 pmol/well). After 24 h, the cells were reseeded in a 24-well plate and cultured in 5% CO_2 at 37°C for an additional 24 h. Subsequently, cells were treated with isotonic or 200 mM NaCl-supplemental medium in 5% CO_2 at 37°C for 12 h and washed with PBS and then stained with crystal violet. The wells were washed with water and air-dried and the dye was eluted with water-containing 0.5% SDS. The absorbance was measured at 590 nm using a Bio-Rad SmartSpec 3000 spectrophotometer (Bio-Rad Laboratories, CA), according to the method reported by Omura et al. (56).

Electroporation

For RNF183 rescue experiments using electroporation, mIMCD-3 cells were transfected with RNF183 or NC siRNA in 10 cm dishes (62.5 pmol/dish). After 12 h, the cells were trypsinized and resuspended in DMEM/F12. They were then pelleted at 1,000 rpm for 5 min and resuspended in OptiMEM at a working concentration of approximately 1.0×10^7 cells/mL. One hundred microliters of cell suspension was added to 10 μg of empty or

3×FLAG-RNF183-pcDNA vectors in electroporation cuvettes (cat# SE-202, BEX Co., Ltd., Tokyo, Japan), then transfected by one direct-current 150 V electrical pulse and five direct-current 20 V electrical pulses at intervals of 50 ms using an electroporator (CUY 21 Vitro-EX, BEX Co., Ltd.). After 48 h, cells were treated with 200 mM NaCl in DMEM/F-12 for the indicated time, and analyzed using western blot or crystal violet assay.

Statistical analysis

Results are expressed as the mean ± standard deviation. Statistical evaluation was performed using JMP statistical software (version Pro 12). Comparisons between two groups were analyzed using the two-tailed *t* test. For multiple group comparisons, one-way analysis of variance (ANOVA), followed by two-tailed Student's *t* test with Bonferroni correction were applied. Significant *P* values of < 0.05, 0.01, or 0.001 are described as $*P < 0.05$, $**P < 0.01$, and $***P < 0.001$, respectively, and nonsignificant *P* values are described as N.S. $P > 0.05$.

Acknowledgments: We appreciate the advice and expertise of Isao Naguro, Shigehiro Doi, Ayumu Nakashima, Toshiki Doi, Shuma Hirashio, and Kensuke Sasaki. We sincerely appreciate Keiji Tanimoto for handling equipment for the hypoxia experiment. Sincere appreciation is extended to Ryoji Kojima for supplying mIMCD-3 cells. Gratitude is expressed to Dr. Takashi Ito and Dr. B. C. Ko for their generous donation of the expression vector pFLAG-NFAT5 and pFLAG-DN-NFAT5. We are grateful to Takeshi Ike and Yui Tanita for their assistance. A part of this work was performed at the Analysis Center of Life Science, Natural Science Center for Basic Research and Development, Hiroshima University. The authors would like to thank Enago (www.enago.jp) for providing an English language review.

Conflict of interest: The authors declare that they have no conflicts of interest with the contents of this article.

Author contributions: MK and YM conceptualized the study; YM performed formal analysis; MK and KI acquired funding; YM performed investigation; SK, TO, AS, RA, and KM designed the methodology; KI overlooked project administration; TM supervised the study; YM, YW, and XG performed data validation; YM performed visualization of cells and tissues; YM and MK wrote the original draft; and KI, TO, and SK reviewed and edited the manuscript.

References

1. Bankir, L., Bouby, N., and Trinh-Trang-Tan, M. M. (1989) The role of the kidney in the maintenance of water balance. *Baillieres. Clin. Endocrinol. Metab.* **3**, 249-311
2. Jamison, R. L. and Kriz, W. (1982) *Urinary concentrating mechanism: structure and function*, Oxford University Press, Oxford, NY
3. Rim, J. S., Atta, M. G., Dahl, S. C., Berry, G. T., Handler, J. S., and Kwon, H. M. (1998) Transcription of the sodium/myo-inositol cotransporter gene is regulated by multiple tonicity-responsive enhancers spread over 50 kilobase pairs in the 5′-flanking region. *J. Biol. Chem.* **273**, 20615-20621
4. Miyakawa, H., Woo, S. K., Dahl, S. C., Handler, J. S., and Kwon, H. M. (1999) Tonicity-responsive enhancer binding protein, a rel-like protein that stimulates transcription in response to hypertonicity. *Proc. Natl. Acad. Sci. U.S.A.* **96**, 2538-2542
5. Ko, B. C., Ruepp, B., Bohren, K. M., Gabbay, K. H., and Chung, S. S. (1997) Identification and characterization of multiple osmotic response sequences in the human aldose reductase gene. *J. Biol. Chem.* **272**, 16431-16437
6. López-Rodríguez, C., Antos, C. L., Shelton, J. M., Richardson, J. A., Lin, F., Novobrantseva, T. I., Bronson, R. T., Igarashi, P., Rao, A., and Olson, E. N. (2004) Loss of NFAT5 results in renal atrophy and lack of tonicity-responsive gene expression. *Proc. Natl. Acad. Sci. U.S.A.* **101**, 2392-2397
7. Woo, S. K., Lee, S. D., Na, K. Y., Park, W. K., and Kwon, H. M. (2002) TonEBP/NFAT5 stimulates transcription of HSP70 in response to hypertonicity. *Mol. Cell. Biol.* **22**, 5753-5760
8. Heo, J. I., Lee, M. S., Kim, J. H., Lee, J. S., Kim, J., Park, J. B., Lee, J. Y., Han, J. A., and Kim, J. I. (2006) The role of tonicity responsive enhancer sites in the transcriptional regulation of human hsp70-2 in response to hypertonic stress. *Exp. Mol. Med.* **38**, 295-301
9. Ito, T., Fujio, Y., Hirata, M., Takatani, T., Matsuda, T., Muraoka, S., Takahashi, K., and Azuma, J. (2004) Expression of taurine transporter is regulated through the TonE (tonicity-responsive element)/TonEBP (TonE-binding protein) pathway and contributes to cytoprotection in HepG2 cells. *Biochem. J.* **382**, 177-182
10. López-Rodríguez, C., Aramburu, J., Jin, L., Rakeman, A. S., Michino, M., and Rao, A. (2001) Bridging the NFAT and NF-kappaB families: NFAT5 dimerization regulates cytokine gene transcription in response to osmotic stress. *Immunity* **15**, 47-58
11. Buxadé, M., Lunazzi, G., Minguillón, J., Iborra, S., Berga-Bolaños, R., Del Val, M., Aramburu, J., and López-Rodríguez, C. (2012) Gene expression induced by Toll-like receptors in macrophages requires the transcription factor NFAT5. *J. Exp. Med.* **209**, 379-393
12. Chen, S., Grigsby, C. L., Law, C. S., Ni, X., Nekrep, N., Olsen, K., Humphreys, M. H., and Gardner, D. G. (2009) Tonicity-dependent induction of Sgk1 expression has a potential role in dehydration-induced natriuresis in rodents. *J. Clin. Invest.* **119**, 1647-1658

13. Kleinewietfeld, M., Manzel, A., Titze, J., Kvakan, H., Yosef, N., Linker, R. A., Muller, D. N., and Hafler, D. A. (2013) Sodium chloride drives autoimmune disease by the induction of pathogenic TH17 cells. *Nature* **496**, 518-522
14. Ito, T., Asakura, K., Tougou, K., Fukuda, T., Kubota, R., Nonen, S., Fujio, Y., and Azuma, J. (2007) Regulation of cytochrome P450 2E1 under hypertonic environment through TonEBP in human hepatocytes. *Mol. Pharmacol.* **72**, 173-181
15. Machnik, A., Neuhofer, W., Jantsch, J., Dahlmann, A., Tammela, T., Machura, K., Park, J. K., Beck, F. X., Müller, D. N., Derer, W., Goss, J., Ziomber, A., Dietsch, P., Wagner, H., van Rooijen, N., Kurtz, A., Hilgers, K. F., Alitalo, K., Eckardt, K. U., Luft, F. C., Kerjaschki, D., and Titze, J. (2009) Macrophages regulate salt-dependent volume and blood pressure by a vascular endothelial growth factor-C-dependent buffering mechanism. *Nat. Med.* **15**, 545-552
16. Hershko, A. and Ciechanover, A. (1998) The ubiquitin system. *Annu. Rev. Biochem.* **67**, 425-479
17. Grabbe, C., Husnjak, K., and Dikic, I. (2011) The spatial and temporal organization of ubiquitin networks. *Nat. Rev. Mol. Cell. Biol.* **12**, 295-307
18. Nakamura, N. (2011) The role of the transmembrane RING finger proteins in cellular and organelle function. *Membranes (Basel)* **1**, 354-393
19. Yu, Q., Zhang, S., Chao, K., Feng, R., Wang, H., Li, M., Chen, B., He, Y., Zeng, Z., and Chen, M. (2016) E3 ubiquitin ligase RNF183 is a novel regulator in inflammatory bowel disease. *J. Crohn's Colitis* **10**, 713-725
20. Geng, R., Tan, X., Wu, J., Pan, Z., Yi, M., Shi, W., Liu, R., Yao, C., Wang, G., Lin, J., Qiu, L., Huang, W., and Chen, S. (2017) RNF183 promotes proliferation and metastasis of colorectal cancer cells via activation of NF-κB-IL-8 axis. *Cell Death Dis.* **8**, e2994
21. Kaneko, M., Iwase, I., Yamasaki, Y., Takai, T., Wu, Y., Kanemoto, S., Matsuhisa, K., Asada, R., Okuma, Y., Watanabe, T., Imaizumi, K., and Nomura, Y. (2016) Genome-wide identification and gene expression profiling of ubiquitin ligases for endoplasmic reticulum protein degradation. *Sci. Rep.* **6**, 30955
22. Woo, S. K., Lee, S. D., and Kwon, H. M. (2002) TonEBP transcriptional activator in the cellular response to increased osmolality. *Pflugers Arch.* **444**, 579-585
23. Ko, B. C., Turck, C. W., Lee, K. W., Yang, Y., and Chung, S. S. (2000) Purification, identification, and characterization of an osmotic response element binding protein. *Biochem. Biophys. Res. Commun.* **270**, 52-61
24. Dahl, S. C., Handler, J. S., and Kwon, H. M. (2001) Hypertonicity-induced phosphorylation and nuclear localization of the transcription factor TonEBP. *Am. J. Physiol. Cell. Physiol.* **280**, C248-253
25. Shapiro, L., and Dinarello, C. A. (1995) Osmotic regulation of cytokine synthesis in vitro. *Proc Natl Acad Sci U S A* **92**, 12230-12234
26. Jantsch, J., Schatz, V., Friedrich, D., Schröder, A., Kopp, C., Siegert, I., Maronna, A., Wendelborn, D.,

Linz, P., Binger, K. J., Gebhardt, M., Heinig, M., Neubert, P., Fischer, F., Teufel, S., David, J. P., Neufert, C., Cavallaro, A., Rakova, N., Küper, C., Beck, F. X., Neuhofer, W., Muller, D. N., Schuler, G., Uder, M., Bogdan, C., Luft, F. C., and Titze, J. (2015) Cutaneous Na+ storage strengthens the antimicrobial barrier function of the skin and boosts macrophage-driven host defense. *Cell Metab* **21**, 493-501

27. Ovcharenko, I., Nobrega, M. A., Loots, G. G., and Stubbs, L. (2004) ECR Browser: a tool for visualizing and accessing data from comparisons of multiple vertebrate genomes. *Nucleic Acids Res.* **32**, W280-286
28. Bryne, J. C., Valen, E., Tang, M. H., Marstrand, T., Winther, O., da Piedade, I., Krogh, A., Lenhard, B., and Sandelin, A. (2008) JASPAR, the open access database of transcription factor-binding profiles: new content and tools in the 2008 update. *Nucleic Acids Res.* **36**, D102-106
29. Santos, B. C., Chevaile, A., Hébert, M. J., Zagajeski, J., and Gullans, S. R. (1998) A combination of NaCl and urea enhances survival of IMCD cells to hyperosmolality. *Am J Physiol* **274**, F1167-1173
30. Michea, L., Ferguson, D. R., Peters, E. M., Andrews, P. M., Kirby, M. R., and Burg, M. B. (2000) Cell cycle delay and apoptosis are induced by high salt and urea in renal medullary cells. *Am J Physiol Renal Physiol* **278**, F209-218
31. Dmitrieva, N., Kultz, D., Michea, L., Ferraris, J., and Burg, M. (2000) Protection of renal inner medullary epithelial cells from apoptosis by hypertonic stress-induced p53 activation. *J Biol Chem* **275**, 18243-18247
32. Alfieri, R. R., Cavazzoni, A., Petronini, P. G., Bonelli, M. A., Caccamo, A. E., Borghetti, A. F., and Wheeler, K. P. (2002) Compatible osmolytes modulate the response of porcine endothelial cells to hypertonicity and protect them from apoptosis. *J Physiol* **540**, 499-508
33. Shim, E. H., Kim, J. I., Bang, E. S., Heo, J. S., Lee, J. S., Kim, E. Y., Lee, J. E., Park, W. Y., Kim, S. H., Kim, H. S., Smithies, O., Jang, J. J., Jin, D. I., and Seo, J. S. (2002) Targeted disruption of hsp70.1 sensitizes to osmotic stress. *EMBO Rep* **3**, 857-861
34. Choudhury, N. R., de Lima Alves, F., de Andrés-Aguayo, L., Graf, T., Cáceres, J. F., Rappsilber, J., and Michlewski, G. (2013) Tissue-specific control of brain-enriched miR-7 biogenesis. *Genes Dev.* **27**, 24-38
35. Berga-Bolaños, R., Drews-Elger, K., Aramburu, J., and López-Rodríguez, C. (2010) NFAT5 regulates T lymphocyte homeostasis and CD24-dependent T cell expansion under pathologic hypernatremia. *J. Immunol.* **185**, 6624-6635
36. Berga-Bolaños, R., Alberdi, M., Buxadé, M., Aramburu, J., and López-Rodríguez, C. (2013) NFAT5 induction by the pre-T-cell receptor serves as a selective survival signal in T-lymphocyte development. *Proc. Natl. Acad. Sci. U.S.A.* **110**, 16091-16096
37. Cha, J. H., Woo, S. K., Han, K. H., Kim, Y. H., Handler, J. S., Kim, J., and Kwon, H. M. (2001) Hydration status affects nuclear distribution of transcription factor tonicity responsive enhancer

binding protein in rat kidney. *J. Am. Soc. Nephrol.* **12**, 2221-2230

38. Sheen, M. R., Kim, J. A., Lim, S. W., Jung, J. Y., Han, K. H., Jeon, U. S., Park, S. H., Kim, J., and Kwon, H. M. (2009) Interstitial tonicity controls TonEBP expression in the renal medulla. *Kidney Int.* **75**, 518-525
39. Hasler, U., Jeon, U. S., Kim, J. A., Mordasini, D., Kwon, H. M., Féraille, E., and Martin, P. Y. (2006) Tonicity-responsive enhancer binding protein is an essential regulator of aquaporin-2 expression in renal collecting duct principal cells. *J Am Soc Nephrol* **17**, 1521-1531
40. Na, K. Y., Woo, S. K., Lee, S. D., and Kwon, H. M. (2003) Silencing of TonEBP/NFAT5 transcriptional activator by RNA interference. *J Am Soc Nephrol* **14**, 283-288
41. Lanaspa, M. A., Andres-Hernando, A., Li, N., Rivard, C. J., Cicerchi, C., Roncal-Jimenez, C., Schrier, R. W., and Berl, T. (2010) The expression of aquaporin-1 in the medulla of the kidney is dependent on the transcription factor associated with hypertonicity, TonEBP. *J Biol Chem* **285**, 31694-31703
42. Brezis, M. and Rosen, S. (1995) Hypoxia of the renal medulla--its implications for disease. *N. Engl. J. Med.* **332**, 647-655
43. Forsythe, J. A., Jiang, B. H., Iyer, N. V., Agani, F., Leung, S. W., Koos, R. D., and Semenza, G. L. (1996) Activation of vascular endothelial growth factor gene transcription by hypoxia-inducible factor 1. *Mol. Cell. Biol.* **16**, 4604-4613
44. Lee, S. D., Choi, S. Y., Lim, S. W., Lamitina, S. T., Ho, S. N., Go, W. Y., and Kwon, H. M. (2011) TonEBP stimulates multiple cellular pathways for adaptation to hypertonic stress: organic osmolyte-dependent and -independent pathways. *Am J Physiol Renal Physiol* **300**, F707-715
45. Maxfield, K. E., Taus, P. J., Corcoran, K., Wooten, J., Macion, J., Zhou, Y., Borromeo, M., Kollipara, R. K., Yan, J., Xie, Y., Xie, X. J., and Whitehurst, A. W. (2015) Comprehensive functional characterization of cancer-testis antigens defines obligate participation in multiple hallmarks of cancer. *Nat. Commun.* **6**, 8840
46. Hasler, U., Leroy, V., Jeon, U. S., Bouley, R., Dimitrov, M., Kim, J. A., Brown, D., Kwon, H. M., Martin, P. Y., and Féraille, E. (2008) NF-kappaB modulates aquaporin-2 transcription in renal collecting duct principal cells. *J. Biol. Chem.* **283**, 28095-28105
47. Roth, I., Leroy, V., Kwon, H. M., Martin, P. Y., Féraille, E., and Hasler, U. (2010) Osmoprotective transcription factor NFAT5/TonEBP modulates nuclear factor-kappaB activity. *Mol. Biol. Cell* **21**, 3459-3474
48. Cheung, C. Y. and Ko, B. C. (2013) NFAT5 in cellular adaptation to hypertonic stress - regulations and functional significance. *J. Mol. Signal.* **8**, 5
49. Lang, F., Busch, G. L., Ritter, M., Völkl, H., Waldegger, S., Gulbins, E., and Häussinger, D. (1998) Functional significance of cell volume regulatory mechanisms. *Physiol. Rev.* **78**, 247-306
50. Petronini, P. G., Alfieri, R. R., Losio, M. N., Caccamo, A. E., Cavazzoni, A., Bonelli, M. A., Borghetti, A. F., and Wheeler, K. P. (2000) Induction of BGT-1 and amino acid system A transport activities in

endothelial cells exposed to hyperosmolarity. *Am. J. Physiol. Regul. Integr. Comp. Physiol.* **279**, R1580-1589

51. Hicke, L. (2001) A new ticket for entry into budding vesicles-ubiquitin. *Cell* **106**, 527-530
52. Hong, J. H., Kaustov, L., Coyaud, E., Srikumar, T., Wan, J., Arrowsmith, C., and Raught, B. (2015) KCMF1 (potassium channel modulatory factor 1) Links RAD6 to UBR4 (ubiquitin N-recognin domain-containing E3 ligase 4) and lysosome-mediated degradation. *Mol. Cell. Proteomics* **14**, 674-685
53. Holleman, J. and Marchese, A. (2014) The ubiquitin ligase deltex-3l regulates endosomal sorting of the G protein-coupled receptor CXCR4. *Mol. Biol. Cell* **25**, 1892-1904
54. Wu, Y., Guo, X. P., Kanemoto, S., Maeoka, Y., Saito, A., Asada, R., Matsuhisa, K., Ohtake, Y., Imaizumi, K., and Kaneko, M. (2018) Sec16A, a key protein in COPII vesicle formation, regulates the stability and localization of the novel ubiquitin ligase RNF183. *PLoS One* **13**, e0190407
55. Bell, L. M., Leong, M. L., Kim, B., Wang, E., Park, J., Hemmings, B. A., and Firestone, G. L. (2000) Hyperosmotic stress stimulates promoter activity and regulates cellular utilization of the serum- and glucocorticoid-inducible protein kinase (Sgk) by a p38 MAPK-dependent pathway. *J. Biol. Chem.* **275**, 25262-25272
56. Omura, T., Kaneko, M., Okuma, Y., Orba, Y., Nagashima, K., Takahashi, R., Fujitani, N., Matsumura, S., Hata, A., Kubota, K., Murahashi, K., Uehara, T., and Nomura, Y. (2006) A ubiquitin ligase HRD1 promotes the degradation of Pael receptor, a substrate of Parkin. *J Neurochem* **99**, 1456-1469

FOOTNOTES:

This study was supported by Grants-in-Aid for Scientific Research (KAKENHI) 17H06416, 15K21706, and 26460099 from the Ministry of Education, Culture, Sports, Science and Technology, Japan and also supported by the Takeda Science Foundation.

The abbreviations used are: RNF, RING finger protein; NFAT5, nuclear factor of activated T-cells 5; AR, aldose reductase; BGT1, sodium- and chloride-dependent betaine transporter; SMIT, sodium myo-inositol co-transporter; HSP70, heat shock protein 70; IBD, inflammatory bowel disease; HEK293, human embryonic kidney 293; TfR, transferrin receptor; qRT-PCR, quantitative real-time RT-PCR; mIMCD-3, mouse inner medullary collecting duct; NRK, normal rat kidney; NC, negative control; ECR, evolutionary conserved region; bp, base pair; miR-7, microRNA-7; VEGFA, vascular endothelial growth factor A ; HIF-1, hypoxia-inducible factor 1; FATE1, fetal and adult testis expressed 1; BIK, Bcl-2-interacting killer; DMEM, Dulbecco's Modified Eagle's Medium; DMEM-F12, DMEM/Nutrient Mixture F-12.

Table 1. Conserved putative transcription factor binding sites in the *RNF183* enhancer region.

Species	Gene	JASPAR Score	Relative Score	Start	End	Strand	Predicted site sequence
Mus musculus	NFIC	8.520	96.1%	−3407	−3402	1	TTGGCT
	ZNF354C	8.723	99.2%	−3398	−3393	1	CTCCAC
	NFE2L1-MafG	8.072	96.8%	−3385	−3380	1	TATGAC
	NFAT	**11.360**	**100.0%**	**−3338**	**−3332**	**1**	**TTTTCCA**
	Atoh1	13.740	99.6%	−3333	−3326	1	CAGCTGGC
	Prrx2	9.124	100.0%	−3299	−3295	1	AATTA
Rattus norvegicus	NFIC	8.520	96.1%	−1935	−1930	1	TTGGCT
	ZNF354C	8.723	99.2%	−1926	−1921	1	CTCCAC
	NFE2L1-MafG	8.812	100.0%	−1913	−1908	1	CATGAC
	NFAT	**11.360**	**100.0%**	**−1866**	**−1860**	**1**	**TTTTCCA**
	Atoh1	13.740	99.6%	−1861	−1854	1	CAGCTGGC
	Prrx2	9.124	100.0%	−1826	−1822	1	AATTA
Homo sapiens	NFIC	8.520	96.1%	−4322	−4317	1	TTGGCT
	ZNF354C	8.723	99.2%	−4313	−4308	1	CTCCAC
	NFE2L1-MafG	8.812	100.0%	−4300	−4295	1	CATGAC
	NFAT	**11.360**	**100.0%**	**−4252**	**−4246**	**1**	**TTTTCCA**
	Atoh1	14.033	100.0%	−4247	−4240	1	CAGATGGC
	Prrx2	9.124	100.0%	−4208	−4204	1	AATTA

Transcription factor-binding sites predicted using the JASPAR software (http://jaspar.genereg.net/) are shown in the mammalian conserved region of *RNF183* genes (mouse, −3,466 to −3,136; rat, −1,978 to −1,664; human, −4,367 to −4,049). Conserved binding sites from mouse, rat, and human were selected from the potential binding sites with a >95% chance (relative score) of binding to any of the listed transcription factors (Table S1). The conserved NFAT5 DNA binding site is indicated in bold.

NFIC, nuclear factor 1 C-type; ZNF354C, zinc finger protein 354C; NFE2L1-MafG, nuclear factor erythroid 2-related factor 1 and V-maf avian musculoaponeurotic fibrosarcoma oncogene homolog G complex; NFAT, nuclear factor of activated T cells; Atoh1, Atonal homolog1; Prrx2, Paired-Related Homeobox 2.

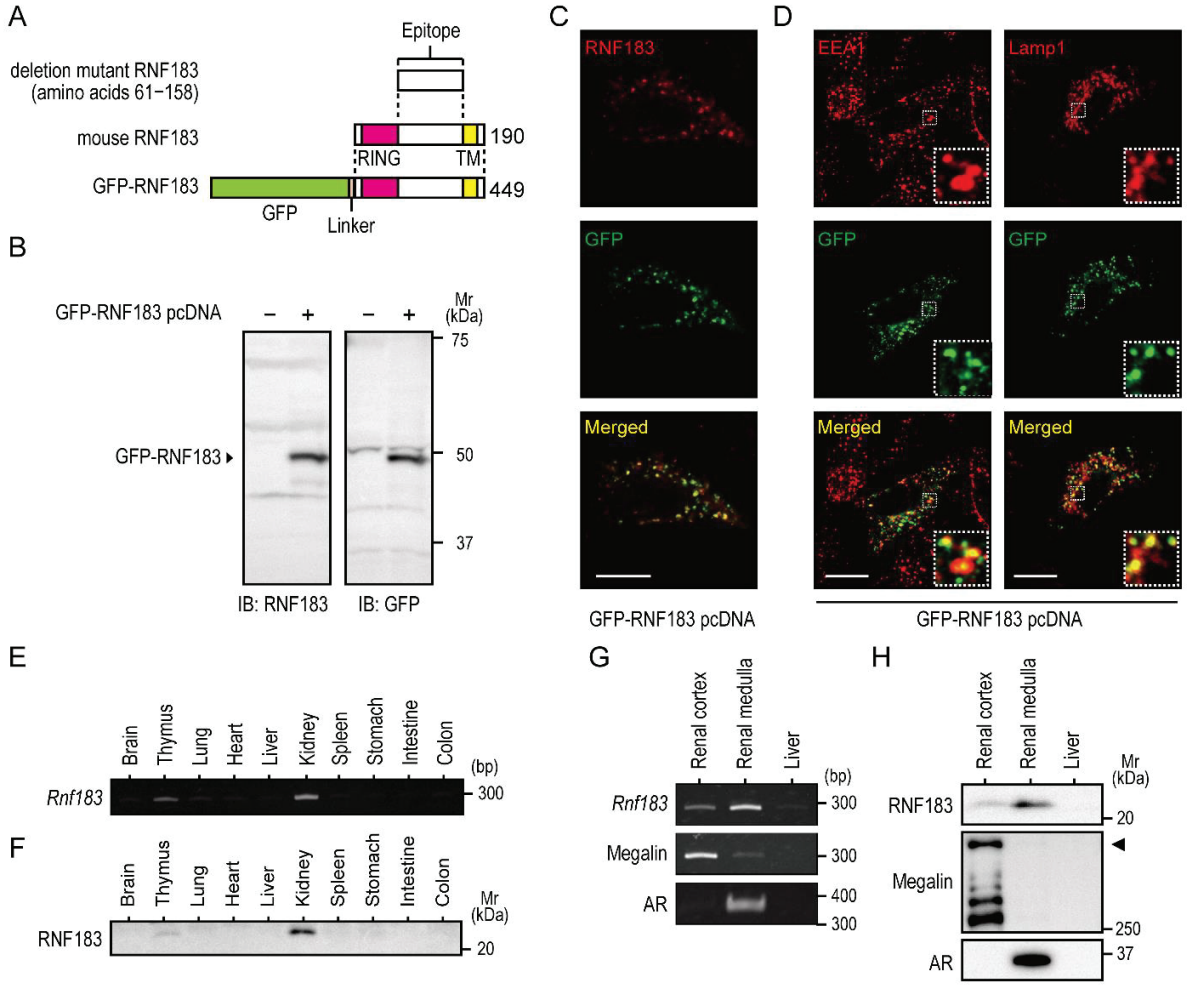

Figure 1. RNF183 is predominantly expressed in the renal medulla. A. Schematic representation of the predicted domain organization of mouse RNF183 (*middle*), deletion mutant RNF183 (amino acids 61–158) (*top*), and GFP-RNF183 (*bottom*) used in this study. Anti-RNF183 antibody was generated using deletion mutant RNF183. The number at *right* indicates the peptide length. **B.** Western blot of HEK-293 cells transfected with GFP-RNF183. The anti-RNF183 and GFP antibody recognized a GFP-RNF183 at approximately 50 kDa. **C.** The confocal images of immunofluorescence with anti-RNF183 antibody (*upper panel, red*) and GFP signals (*middle panel, green*) in HeLa cells transfected with GFP-RNF183. Bar: 10 μm. **D.** The confocal images of immunofluorescence with GFP signals (*middle panels, green*) and various antibodies for organelle markers (EEA1 and Lamp1; *upper panels, red*) in HeLa cells transfected with GFP-RNF183. Bars, 10 μm. **E.** RT-PCR analysis of *Rnf183* mRNA in 10 tissues from mice. **F.** Tissue immunoblot analysis of RNF183. Tissue lysates containing equal amount of total protein were analyzed by western blot. **G and H.** Expression patterns of RNF183 mRNA and protein in the renal cortex and medulla. Mouse tissue lysates were analyzed by RT-PCR **(G)** and western blot **(H)**. Liver was used as a negative control. Megalin and AR were used as positive controls for the renal cortex and medulla,

respectively. Arrow head indicates full-length Megalin (**H,** *middle panel*). The results shown are representative of at least three replicates in independent observations.

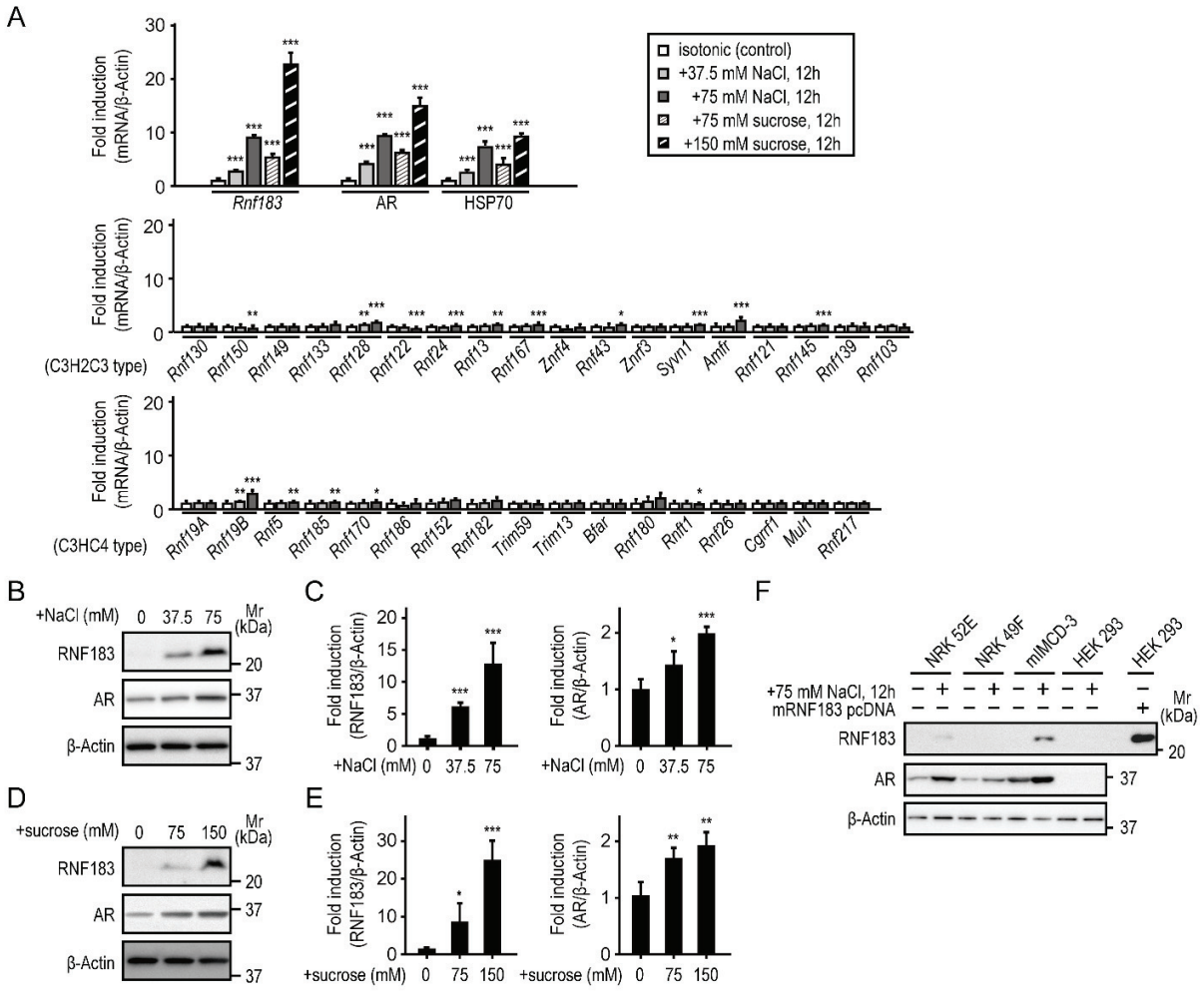

Figure 2. RNF183 is upregulated in response to hypertonic stress. A. The hypertonic response of *Rnf183* (*top*) and the other transmembrane RNF family member (*middle*, 18 of C3H2C3 type; *bottom*, 17 of C3HC4 type) mRNA levels in mIMCD-3 cells. AR and HSP70 were used as tonicity-dependent positive controls (*top*). Cells were treated with isotonic or indicated NaCl- or sucrose-supplemented medium for 12 h and analyzed by qRT-PCR (n = 5). **B and D.** The tonicity-dependent induction of RNF183 and AR protein in mIMCD-3 cells. Cells were cultured under hypertonic conditions by adding indicated **(B)** NaCl or **(C)** sucrose supplementation for 12 h and analyzed by western blot. **C and E.** Quantitative analysis of RNF183 (*left*) and AR (*right*) protein expression in (**B,** NaCl) and (**D,** sucrose) (n = 5). **F.** The upregulation patterns of RNF183 and AR proteins in four renal cell lines in response to hypertonic stress. NRK-52E, NRK-49F, mIMCD-3, and HEK293 cells were treated with isotonic or 75 mM NaCl-supplemented medium for 12 h and analyzed by western blot. HEK293 cells transfected with mouse RNF183 were used as a positive control. Data were analyzed by one-way ANOVA, followed by the *post hoc* tests using t tests with Bonferroni correction. Values represent mean ± SD. *$P < 0.05$, **$P < 0.01$, or ***$P < 0.001$ (versus isotonic control).

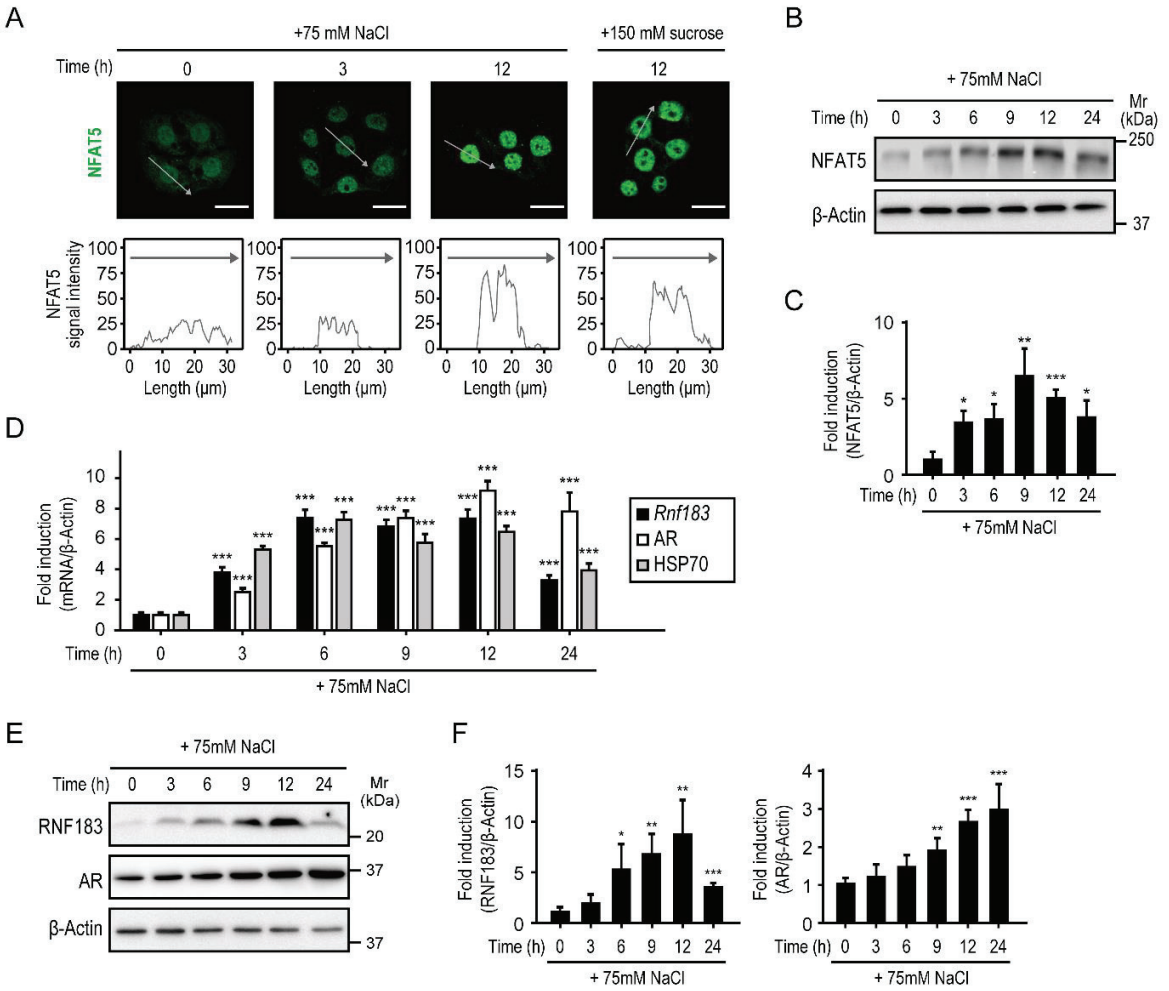

Figure 3. RNF183 is upregulated concurrently with NFAT5 activation. A. The nuclear translocation of NFAT5 in response to hypertonic stress. Mouse IMCD-3 cells were treated with hypertonic medium (75 mM NaCl- or 150 mM sucrose-supplemented medium) for indicated time and subjected to immunofluorescence staining with anti-NFAT5 antibody (*upper panels*, *green*). Bars, 20 μm. The NFAT5 fluorescence intensities of cells were plotted on line graphs (*lower panels*). Gray lines correspond to the relative fluorescence of cells marked with gray arrows. **B.** The increase in total NFAT5 protein abundance in response to hypertonic stress. Mouse IMCD-3 cells were treated with 75 mM NaCl-supplemented medium for indicated time and analyzed by western blot. **C.** Quantification of data from **B** ($n = 4$). **D and E.** Time-course analysis of mRNA and protein in response to hypertonic stress. Mouse IMCD-3 cells were treated with NaCl-supplemented medium for indicated time and analyzed by qRT-PCR (**D,** $n = 6$) or by western blot (**E**). **F.** Quantitative analysis of RNF183 (*left*) and AR (*right*) expression in **E** ($n = 5$). Data were analyzed by one-way ANOVA, followed by the *post hoc* tests using *t* tests with Bonferroni correction. Values represent mean ± SD. *$P < 0.05$, **$P < 0.01$, or ***$P < 0.001$ (versus isotonic control).

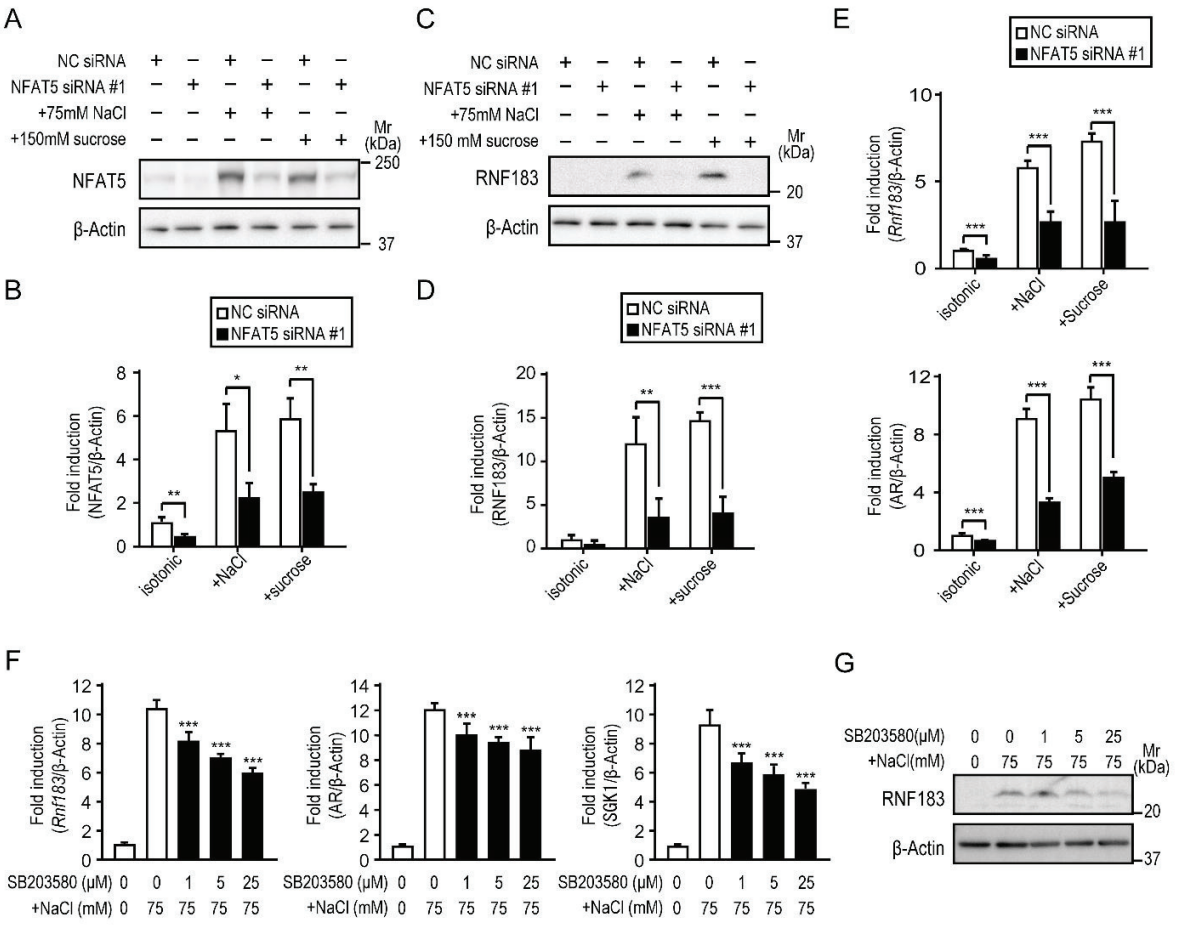

Figure 4. NFAT5 knockdown and p38/MAPK inhibitor SB203580 attenuate hypertonicity-induced RNF183 expression. A. Inhibition of NFAT5 expression using siRNA. Mouse IMCD-3 cells transfected with NFAT5 siRNA #1 or negative control (NC) siRNA were treated with isotonic or 75 mM NaCl- or 150 mM sucrose-supplemented medium for 12 h and analyzed by western blot. **B.** Quantification of data from **A** ($n = 4$). **C.** Effect of NFAT5 knockdown on RNF183 protein expression induced by hypertonicity. **D.** Quantitative analysis of RNF183 in **C** ($n = 4$). **E.** Effect of NFAT5 knockdown on *Rnf183* (*left*) and AR (*right*) mRNA ($n = 5$). **F and G.** Effect of p38/MAPK inhibitor SB203580 on **(F)** mRNA expression of *Rnf183*, AR, and SGK1 and **(G)** protein expression of RNF183. Cells were treated with 75 mM NaCl for 12 h in the presence of indicated concentrations of SB203580 (1 h of preincubation) and analyzed by **(F)** qRT-PCR ($n = 6$) or **(G)** western blot. Data were analyzed by one-way ANOVA, followed by the *post hoc* tests using *t* tests with Bonferroni correction. Values represent mean ± SD. $^{*}P < 0.05$, $^{**}P < 0.01$, or $^{***}P < 0.001$ (versus NC).

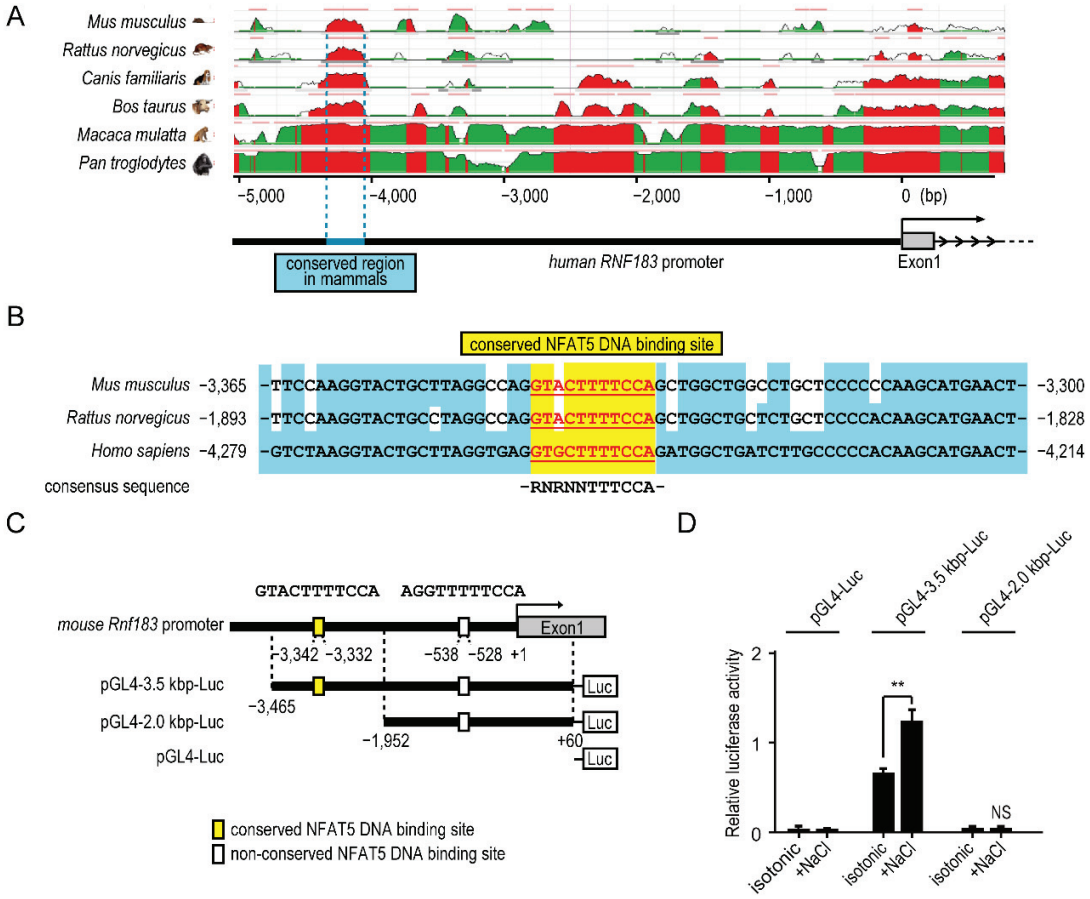

Figure 5. Identification of the *Rnf183* enhancer region that responds to hypertonic stress. A. Screen capture from the ECR Browser web site (http://ecrbrowser.dcode.org/) of the human *RNF183* gene with evolutionary conserved region (ECR) in the genomes of mouse, rat, canis, cattle, rhesus, and chimpanzee. The peaks in red show comparative pairwise ECR between human and indicated mammals. The 319-bp region (−4,367 to −4,049 region; numbers indicate nucleotide positions relative to the transcription start site) is conserved in mammals (*blue*). **B.** Location and sequence of the conserved NFAT5 DNA-binding site (*yellow background with underline*; mouse, −3,342 to −3,332 bp; rat, −1,870 to −1,860 bp; human, −4,256 to −4,246 bp). Conserved bases around the binding site are indicated as *blue background*. NFAT5 consensus sequence (RNRNNTTTCCA) is indicated below the site. **C.** Scheme of the mouse *Rnf183* promoter region and reporter constructs. Two NFAT5 DNA-binding sites are indicated in 3.5 kbp upstream of the mouse *Rnf183* start site. 3.5 kbp-Luc and 2.0 kbp-Luc constructs consist of approximately 3.5 kbp and 2.0 kbp upstream of the mouse *Rnf183* transcription start site, respectively. **D.** Effect of hypertonic stress on luciferase activities. Mouse IMCD-3 cells transfected with 3.5 kbp-Luc or 2.0 kbp-Luc constructs were treated with isotonic or 75 mM NaCl-supplemented medium for 24 h. The pGL4-Luc without the promoter was used as a control. Firefly luciferase activities were normalized to *Renilla* luciferase signals ($n = 3$). Data were analyzed by one-way ANOVA, followed by the *post hoc* tests

using *t* tests with Bonferroni correction. Values represent mean ± SD. **$P < 0.01$ or N.S. $P > 0.05$.

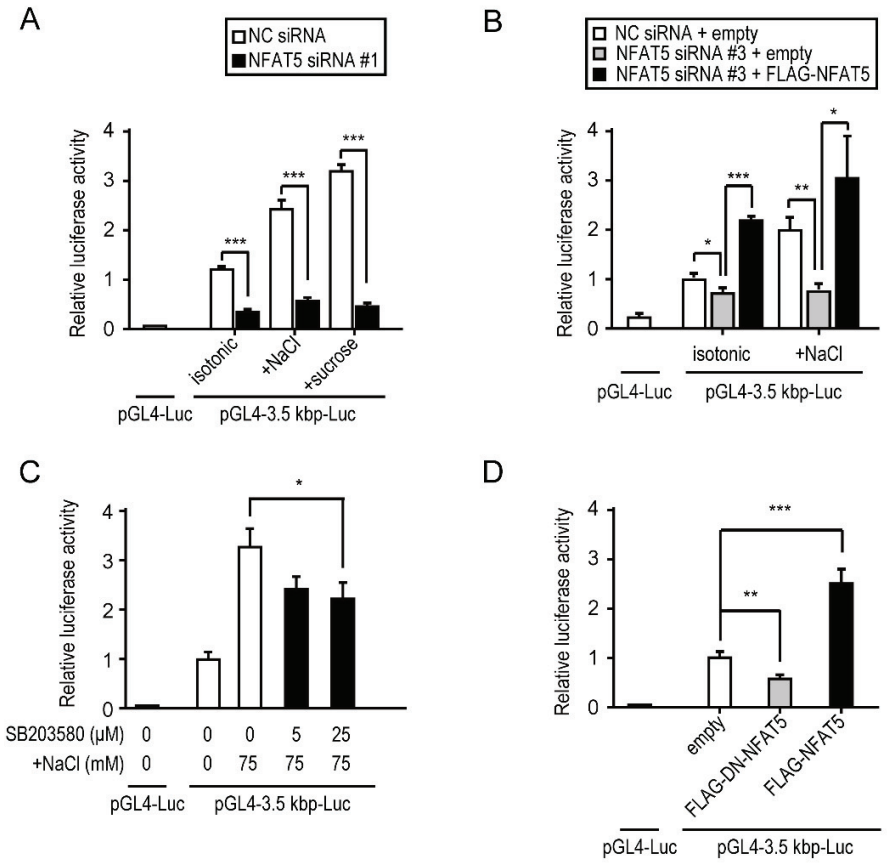

Figure 6. *Rnf183* enhancer region depends on NFAT5. A. Effect of NFAT5 knockdown on hypertonicity-induced luciferase activities. Cells cotransfected with 3.5 kbp-Luc and siRNA (NFAT5 #1 or NC) were treated with isotonic or 75 mM NaCl- or sucrose-supplemented medium for 24 h (n = 3). **B.** Effect of rescue with FLAG-NFAT5 on luciferase activities. Cells pretransfected with siRNA (NFAT5 #3 or NC) were cotransfected with 3.5 kbp-Luc and either empty or pFLAG-NFAT5 vectors after 12 h of knockdown. After 24 h of cotransfection, cells were treated with isotonic or 75 mM NaCl-supplemented medium for an additional 24 h (n = 4). **C.** Effect of p38/MAPK inhibitor SB203580 on *Rnf183* luciferase activities. Cells transfected with 3.5 kbp-Luc were treated with 75 mM NaCl for 24 h in the presence of the indicated concentrations of SB203580 (1 h of preincubation) (n = 3). **D.** Effect of overexpression with FLAG-dominant negative (DN)-NFAT5 and FLAG-NFAT5 on luciferase activities. Cells cotransfected with 3.5 kbp-Luc and either empty, pFLAG-DN-NFAT5, or pFLAG-NFAT5 vectors were analyzed after 48 h of transfection (n = 4). Data were analyzed by one-way ANOVA, followed by the *post hoc* tests using t tests with Bonferroni correction. Values represent mean ± SD. *$P < 0.05$, **$P < 0.01$, or ***$P < 0.001$.

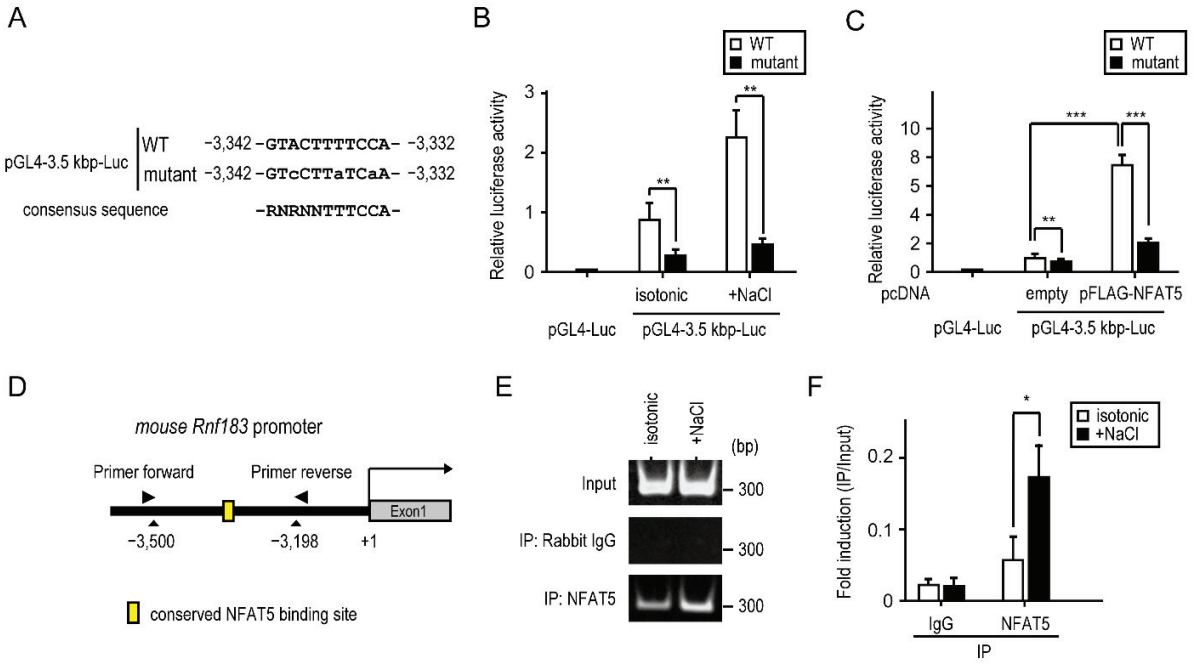

Figure 7. *Rnf183* is a direct target of NFAT5. A. Location and site-directed mutagenesis of the conserved NFAT5 DNA-binding site. The sequences from the pGL4-3.5 kbp-Luc of the WT and mutant are shown. Mutagenized bases are indicated by lower-case letters. **B.** Effect of conserved site mutation on luciferase activities. Cells transfected with WT or mutant were cultured isotonic or 75 mM NaCl-supplemented medium for 24 h. The pGL4-Luc was used as a control. Firefly luciferase activities were normalized to Renilla luciferase signals (n = 4). **C.** Effect of NFAT5 overexpression on luciferase activities. Cells transfected with WT, mutant, empty, or pFLAG-NFAT5 were cultured in an isotonic medium for 36 h. (n = 5). **D.** Schematic representation of the *Rnf183* promoter and the annealing sites of the primer set used in the ChIP assays. **E.** ChIP assay analysis of the NFAT5 binding to the *Rnf183* promoter in mIMCD-3 cells. ChIP assays were performed with the indicated antibodies. Immunoprecipitated (IP) DNA and input DNA were subjected to RT-PCR. IgG was used as a control. **F.** Quantitative analysis of RT-PCR in **E**. Results were normalized to input DNA (n = 3). Data were analyzed by one-way ANOVA, followed by the *post hoc* tests using t tests with Bonferroni correction. Values represent mean ± SD. *$P < 0.05$, **$P < 0.01$, or ***$P < 0.001$ (versus isotonic control).

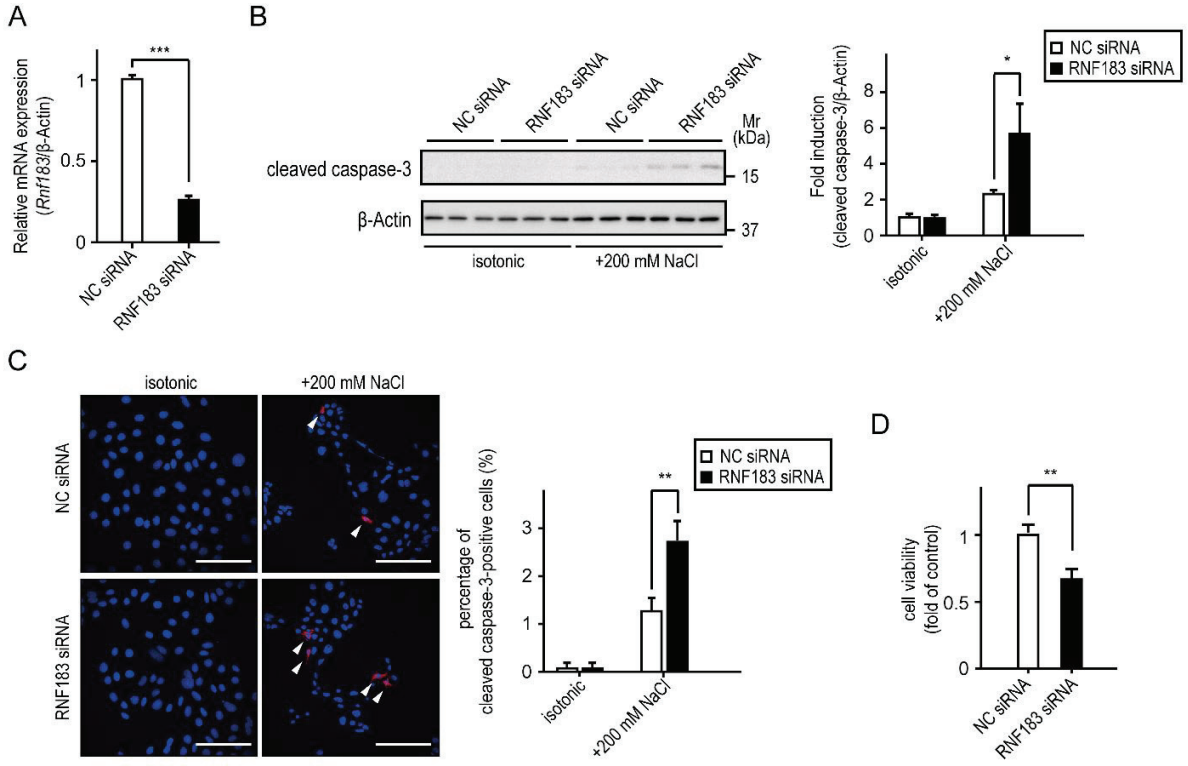

Figure 8. RNF183 expression provides protection against hypertonicity-induced apoptosis A. Inhibition of *Rnf183* expression using siRNA. Mouse IMCD-3 cells transfected with RNF183 siRNA or NC siRNA were analyzed using qRT-PCR (n = 3). **B and C.** Effect of RNF183 knockdown on hypertonicity-induced apoptosis. Cells transfected with the indicated siRNAs were treated with isotonic or 200 mM NaCl-supplemented medium for 4 h and analyzed using **(B)** western blotting or **(C)** immunofluorescence staining using anti-cleaved caspase-3-specific antibody. **B.** The accompanying bar graph summarizes the quantification of relative amounts of cleaved caspase-3 (n = 3). **C.** The cleaved caspase-3 fluorescence-positive cells (*red*) are marked with white arrows. Bars, 100 μm. The number of cleaved caspase-3-positive cells was counted in five different fields of view and divided by the number of DAPI-stained cells (*blue*) to yield the ratio of cleaved caspase-3 positive cells; the results are summarized in the accompanying bar graph (n = 3). **D.** Effect of RNF183 knockdown on cell viability under hypertonic conditions. Cells transfected with the indicated siRNAs were treated with isotonic or 200 mM NaCl-supplemented medium for 12 h, and analyzed using crystal violet assay (n = 3). Data were analyzed using t test **(A and D)** or one-way ANOVA, followed by the *post hoc* tests using t tests with Bonferroni correction **(B and C)**. Values represent mean ± SD. *$P < 0.05$, **$P < 0.01$, or ***$P < 0.001$ (versus NC).

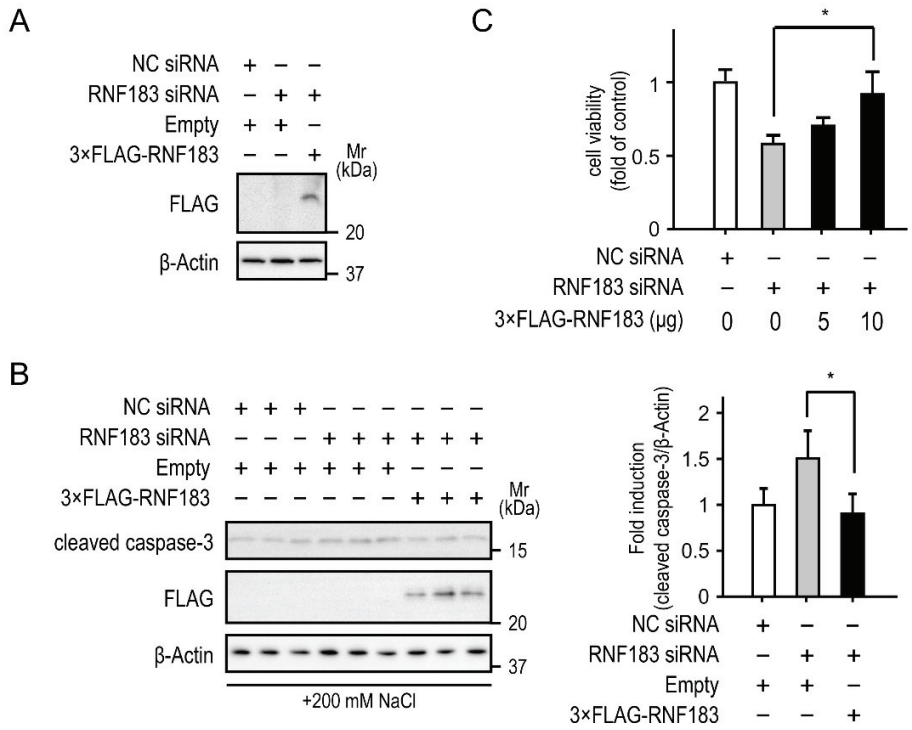

Figure 9. Rescue of RNF183 knockdown attenuates hypertonicity-induced apoptosis. A. Resistance of 3×FLAG-RNF183 to RNF183 siRNA. Mouse IMCD-3 cells were transfected with RNF183 siRNA or NC siRNA. After 12 h, the cells were electroporated with empty or 3×FLAG-RNF183-pcDNA vectors, and were analyzed by western blotting 48 h after electroporation. **B and C.** Effect of rescue of RNF183 knockdown on **(B)** hypertonicity-induced apoptosis and **(C)** cell viability. Cells transfected with RNF183 siRNA or NC siRNA were electroporated with empty or 3×FLAG-RNF183-pcDNA vectors. After 48 h of electroporation, cells were treated with 200 mM NaCl -supplemented medium for **(B)** 4 and **(C)** 12 h, and then analyzed using **(B)** western blot and **(C)** crystal violet assay ($n = 3$), respectively. The accompanying bar graph summarizes the quantification of the relative amounts of cleaved caspase-3 ($n = 3$). Data were analyzed by one-way ANOVA, followed by the *post hoc* tests using *t* tests with Bonferroni correction. Values represent mean ± SD. *$P < 0.05$.

NFAT5 up-regulates expression of the kidney-specific ubiquitin ligase gene *Rnf183* under hypertonic conditions in inner-medullary collecting duct cells

Yujiro Maeoka, Yan Wu, Takumi Okamoto, Soshi Kanemoto, Xiao Peng Guo, Atsushi Saito, Rie Asada, Koji Matsuhisa, Takao Masaki, Kazunori Imaizumi and Masayuki Kaneko

J. Biol. Chem. published online November 9, 2018

NFAT5 up-regulates expression of the kidney-specific ubiquitin ligase gene *Rnf183* under hypertonic conditions in inner-medullary collecting duct cells

Yujiro Maeoka[1,2], Yan Wu[1], Takumi Okamoto[1], Soshi Kanemoto[1,3], Xiao Peng Guo[1], Atsushi Saito[4], Rie Asada[1,5], Koji Matsuhisa[4], Takao Masaki[2], Kazunori Imaizumi[1*], Masayuki Kaneko[1*]

Supporting Information

1. Table S1
2. Figures S1−S6

Table S1. Putative transcription factor binding sites in the *RNF183* enhancer region.

Mus musculus

Gene	JASPAR Score	Relative Score	Start	End	Strand	Predicted site sequence
STAT5	15.281	98.1%	-3466	-3456	1	CTTTCCCAGAA
STAT1	17.040	99.3%	-3465	-3455	-1	TTTCTGGGAAA
STAT3	16.483	99.7%	-3465	-3455	-1	TTTCTGGGAAA
SP1	13.428	95.0%	-3438	-3428	1	CCCCCGCCCCG
KLF5	13.577	97.6%	-3438	-3429	1	CCCCCGCCCC
Mafb	9.499	100.0%	-3430	-3423	-1	GCTGACGG
SP1	13.428	95.0%	-3423	-3413	1	CCCCCGCCCCG
KLF5	13.577	97.6%	-3423	-3414	1	CCCCCGCCCC
NFIC [a]	8.520	96.1%	-3407	-3402	1	TTGGCT
ZNF354C [a]	8.723	99.2%	-3398	-3393	1	CTCCAC
NFE2L1-MafG [a]	8.072	96.8%	-3385	-3380	1	TATGAC
NFAT [a]	11.360	100.0%	-3338	-3332	1	TTTTCCA
Atoh1 [a]	13.740	99.6%	-3333	-3326	1	CAGCTGGC
MZF1_1-4	8.252	96.2%	-3317	-3312	-1	GGGGGA
Lhx3	16.202	96.3%	-3303	-3291	-1	AAATTAATTAGTT
Nobox	10.854	98.3%	-3302	-3295	-1	TAATTAGT
Pdx1	9.570	100.0%	-3301	-3296	1	CTAATT
Prrx2	9.124	100.0%	-3300	-3296	-1	AATTA
Prrx2 [a]	9.124	100.0%	-3299	-3295	1	AATTA
Prrx2	9.124	100.0%	-3296	-3292	-1	AATTA
Stat6	15.738	95.5%	-3283	-3269	1	AAGTTCCTGAGAAGC
Klf1	14.517	95.7%	-3271	-3261	1	AGCCCCACCCT
KLF5	14.984	99.4%	-3270	-3261	1	GCCCCACCCT
Klf4	15.246	99.6%	-3270	-3261	-1	AGGGTGGGGC
GATA3	13.321	97.9%	-3242	-3235	1	AGATAAAA
FOXD1	11.362	96.1%	-3223	-3216	-1	GTAAACAG
FOXO3	11.549	98.0%	-3222	-3215	-1	GGTAAACA
Mafb	8.818	97.0%	-3171	-3164	1	GCTGACTC
NFE2L1-MafG	8.692	99.5%	-3159	-3154	1	GATGAC

Rattus norvegicus

Gene	JASPAR Score	Relative Score	Start	End	Strand	Predicted site sequence
STAT5	14.146	96.7%	-1978	-1968	1	CCTTCCCAGAA
Atoh1	12.065	97.0%	-1972	-1965	1	CAGAAGGC
NFIC [a]	8.520	96.1%	-1935	-1930	1	TTGGCT
ZNF354C [a]	8.723	99.2%	-1926	-1921	1	CTCCAC
NFE2L1-MafG [a]	8.812	100.0%	-1913	-1908	1	CATGAC
NFAT [a]	11.360	100.0%	-1866	-1860	1	TTTTCCA
Atoh1 [a]	13.740	99.6%	-1861	-1854	1	CAGCTGGC
MZF1_1-4	9.085	100.0%	-1845	-1840	-1	TGGGGA
Prrx2 [a]	9.124	100.0%	-1826	-1822	1	AATTA
Prrx2	9.124	100.0%	-1823	-1819	-1	AATTA
HOXA5	8.661	95.8%	-1813	-1806	1	CTCAAATT
MZF1_1-4	9.085	100.0%	-1797	-1792	-1	TGGGGA
GATA3	13.321	97.9%	-1769	-1762	1	AGATAAAA
FOXD1	11.362	96.1%	-1751	-1744	-1	GTAAACAG
FOXO3	12.142	100.0%	-1750	-1743	-1	TGTAAACA
SOX10	8.910	100.0%	-1745	-1740	-1	CTTTGT
NFE2L1-MafG	8.692	99.5%	-1687	-1682	1	GATGAC

Homo sapiens

Gene	JASPAR Score	Relative Score	Start	End	Strand	Predicted site sequence
NFIC [a]	8.520	96.1%	-4322	-4317	1	TTGGCT
ZNF354C [a]	8.723	99.2%	-4313	-4308	1	CTCCAC
NFE2L1-MafG [a]	8.812	100.0%	-4300	-4295	1	CATGAC
Hltf	7.794	95.6%	-4279	-4270	-1	TACCTTAGAC
NFAT [a]	11.360	100.0%	-4252	-4246	1	TTTTCCA
Atoh1 [a]	14.033	100.0%	-4247	-4240	1	CAGATGGC
Pdx1	9.570	100.0%	-4208	-4203	-1	CTAATT
Prrx2 [a]	9.124	100.0%	-4208	-4204	1	AATTA
NFAT	11.360	100.0%	-4151	-4145	-1	TTTTCCA
BRCA1	7.447	95.7%	-4136	-4130	-1	CCAACAG
NFIC	9.697	100.0%	-4133	-4128	1	TTGGCA
HOXA5	9.854	100.0%	-4069	-4062	-1	CACTAATT
Pdx1	9.570	100.0%	-4069	-4064	-1	CTAATT
Prrx2	9.124	100.0%	-4069	-4065	1	AATTA
NFAT	11.360	100.0%	-4058	-4052	-1	TTTTCCA

Transcription factor-binding sites predicted using the JASPAR software (http://jaspar.genereg.net/) are shown in the mammalian conserved region of *RNF183* genes (mouse, −3,466 to −3,136; rat, −1,978 to −1,664; human, −4,367 to −4,049). The potential binding sites with a >95% chance (relative score) of binding to any of the listed transcription factors. [a] Conserved binding sites among mouse, rat, and human. The conserved NFAT5 DNA binding site is indicated as *yellow background*.

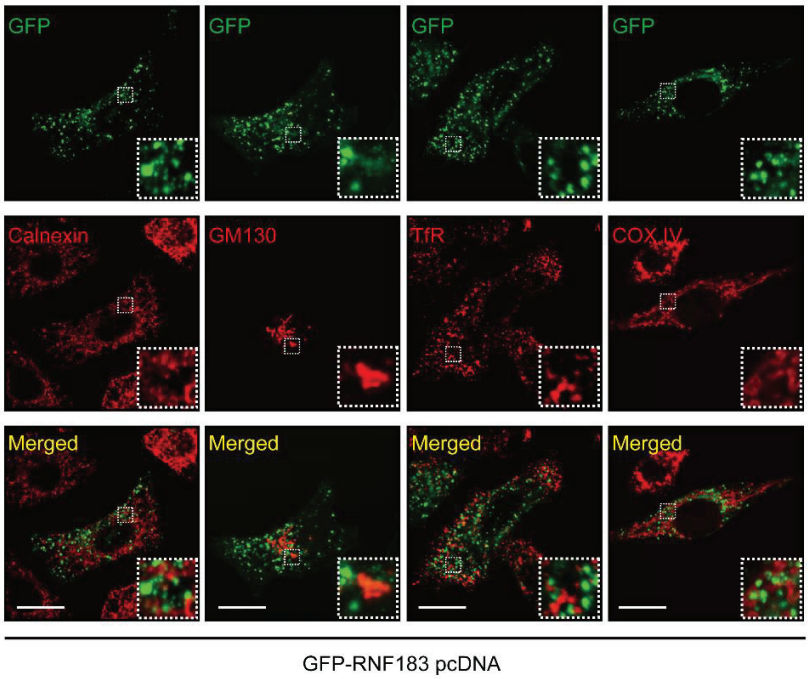

Figure S1. Subcellular localization of RNF183. The confocal images of immunofluorescence with GFP signals (*upper panels, green*) and various antibodies for organelle markers (Calnexin, GM130, TfR, and COX IV; *middle panels, red*) in HeLa cells transfected with GFP-RNF183. Bars, 10 μm. All images shown are representative of at least three replicates in independent observations.

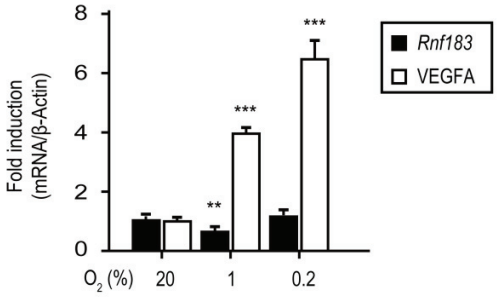

Figure S2. RNF183 expression is not up-regulated under hypoxia. Effect of hypoxia on *Rnf183* expression. Mouse IMCD-3 cells were maintained in hypoxia (0.1% or 0.3% O_2) or normoxia (20% O_2) chambers for 12 h at 37°C and analyzed by qRT-PCR analysis. VEGFA was used as a hypoxia-induced positive control. Expression levels were compared with those in normoxia ($n = 6$). Data were analyzed by one-way ANOVA, followed by the *post hoc* tests using *t* tests with Bonferroni correction. Values represent mean ± SD. $^{**}P < 0.01$, $^{***}P < 0.001$ (versus normoxic control).

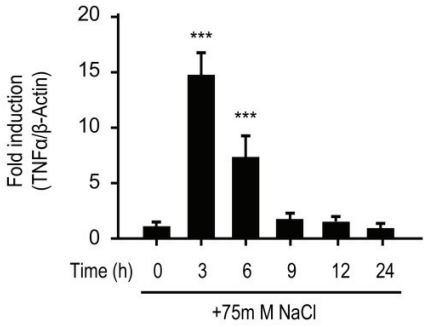

Figure S3. TNFα mRNA peaked after 3h of hypertonic stimulation. Time-course analysis of TNFα mRNA in response to hypertonic stress. Mouse IMCD-3 cells were treated with 75 mM NaCl-supplementation for indicated time and analyzed by qRT-PCR analysis. Expression levels were compared with those in isotonic control ($n = 6$). Data were analyzed by one-way ANOVA followed by the *post hoc* tests using *t* tests with Bonferroni correction. Values represent mean ± S.D. *** $P < 0.001$ (versus isotonic control).

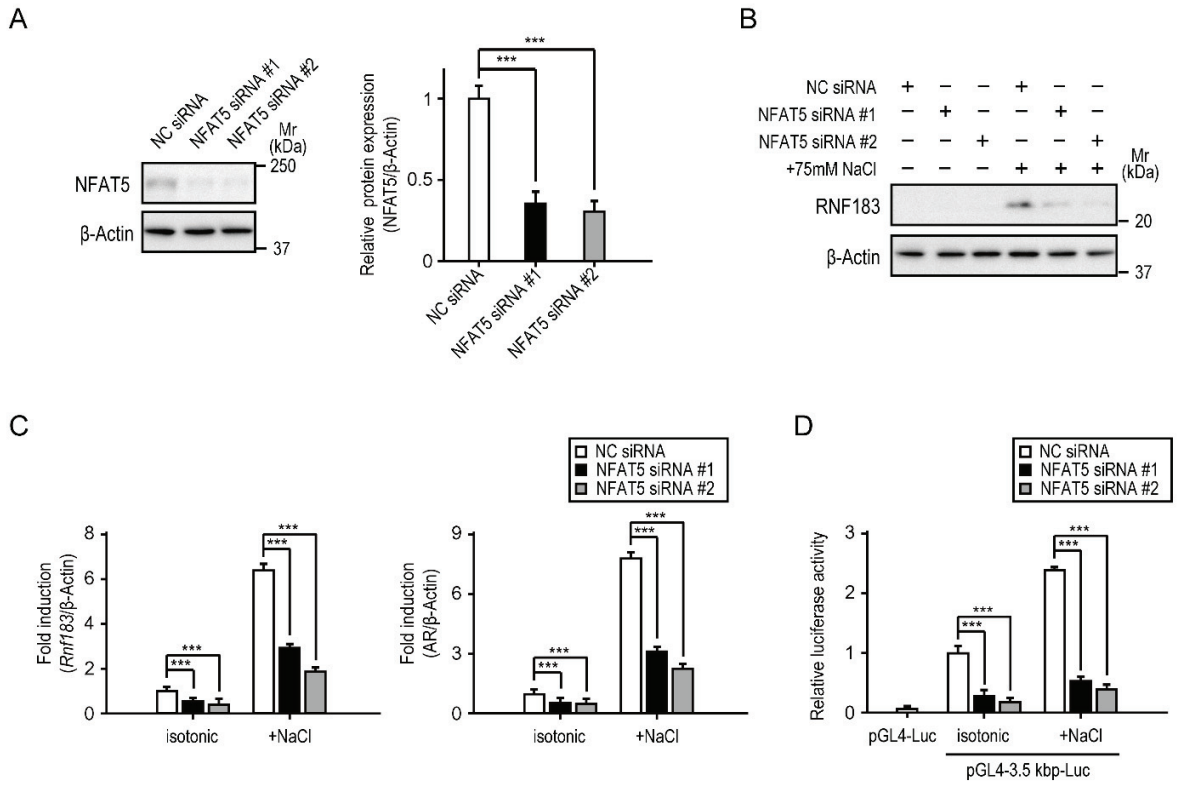

Figure S4. NFAT5 knockdown attenuates hypertonicity-induced RNF183 expression. A. Inhibition of NFAT5 expression using siRNA #2-mediated knockdown. Mouse IMCD-3 cells transfected with NFAT5 siRNA #1, NFAT5 siRNA #2, or negative control (NC) siRNA were analyzed by western blotting. The quantification of NFAT5 is summarized in the accompanying bar graph (n = 3). **B and C.** Effects of NFAT5 siRNA #2-mediated knockdown on **(B)** expression of RNF183 protein and **(C)** expression of *Rnf183* (*left*) and AR (*right*) mRNA (n = 4). mIMCD-3 cells transfected with NFAT5 siRNA #1, NFAT5 siRNA #2, or NC siRNA were treated with isotonic or 75 mM NaCl -supplemented medium for 12 h and analyzed using **(B)** western blot and **(C)** qRT-PCR. **D.** Effect of NFAT5 siRNA #2-mediated knockdown on hypertonicity-induced promoter activities. Cells co-transfected with 3.5 kbp-Luc and siRNA (NFAT5 #1, NFAT5 #2 or NC) were treated with isotonic or 75 mM NaCl- or sucrose-supplemented medium for 24 h (n = 4). Data were analyzed by one-way ANOVA, followed by the *post hoc* tests using t tests with Bonferroni correction. Values represent mean ± SD. ***$P < 0.001$ (versus NC).

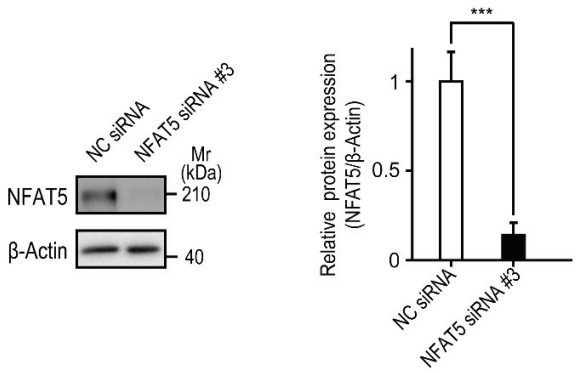

Figure S5. Inhibition of NFAT5 expression using NFAT5 siRNA #3-mediated knockdown. Mouse IMCD-3 cells transfected with NFAT5 siRNA #3 or negative control (NC) siRNA were analyzed by western blotting. The quantification of NFAT5 is summarized in the accompanying bar graph (n = 3). Data were analyzed by t test. Values represent mean ± SD. ***$P < 0.001$.

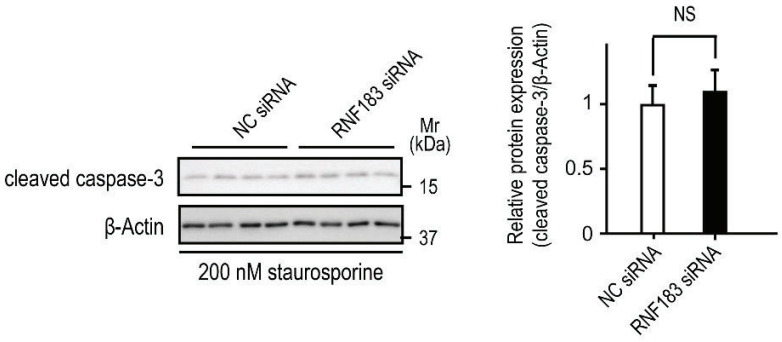

Figure S6. RNF183 expression did not protect against staurosporine-induced apoptosis

Cells transfected with the indicated siRNAs were treated with 200 nM staurosporine-supplemented medium for 12 h and analyzed using western blotting. The accompanying bar graph summarizes the quantification of relative amounts of cleaved caspase-3 (n = 4). Values represent mean ± SD. N.S. P > 0.05 (versus NC).